LAKE LEVEL FORECASTING FOR HYDRO POWER OPERATION IN THE CLUTHA CATCHMENT

A thesis

submitted in partial fulfilment

of the requirements for the degree

of

Master of Science in Earth Sciences

at

The University of Waikato

by

AMY MARGARET WATERS

THE UNIVERSITY OF
WAIKATO
Te Whare Wānanga o Waikato

The University of Waikato

2019

Abstract

The Clutha River is New Zealand's largest river, located within New Zealand's largest catchment. The river runs through two hydro-power stations, the Clyde Dam and downstream the Roxburgh Dam, together providing around 10% of New Zealand's electrical energy. Over 80% of the river flow at Clyde Dam is sourced from the outflow of three large lakes further up in the catchment, Lake Wanaka, Lake Wakatipu and Lake Hāwea. To efficiently operate the hydro-scheme the operator, Contact Energy, requires hourly forecast of the inflows into the head-pond lake of the Clyde Dam, Lake Dunstan. The current model is subject to some degree of predictive error and it has been identified that improving the accuracy of the forecast levels of Lakes Wanaka and Wakatipu may reduce the error of the inflow model.

This project develops an empirical model for estimating the lake level changes, with a lead-time from 1 hour out to 48 hours, in Lakes Wanaka and Wakatipu, using only a few independent variables. The empirical model was developed, calibrated, and first evaluated using recorded rainfall and temperature data (hindcast validation). The model was then revaluated using forecast rainfall and temperature data to gain an understanding of how the model will perform during operation (forecast validation).

The empirical model has two main components, the first component estimates the lake level recession rates as a function of current lake level. The second component estimates the lake rise resulting from recent rainfall in the catchment, the model uses an inverse Gaussian distribution to represent the lake level rise hydrograph form resulting from recent effective rainfall in the catchment. Average catchment temperature is used as a proxy for estimating the proportion of rainfall contributing to lake level rise.

During the hindcast validation the model performed reasonably well, closely estimating the time distribution of positive lake level changes and lake level recessions. For Lakes Wanaka and Wakatipu, the Nash-Sutcliffe efficiency index values for each season, at lead-time of 48 hours, had minimal change from the calibration index values, apart from in spring where the values notably dropped.

To perform the forecast validation, the forecast rainfall was first correlated to recorded rainfall, for which the model was calibrated. The use of weather-based forecasts of rainfall and temperature introduced a significant amount of error. While most of the time the forecast rainfall accurately predicted the presence of rainfall, the forecast rainfall depth was subject to a large error. This transferred through to the model output, with the model largely accurately predicting if the lake level will rise or fall but lost accuracy predicting the magnitude of lake level rises.

For the forecast validation the Nash-Sutcliffe efficiency index values for each season, at a lead-time of 48 hours, all dropped, apart from winter, when compared to the hindcast calibration fits. Again, spring performed the worst for both lakes. The model tended to underpredict most lake levels rises, with the extent of underprediction increasing with increasing predicted lake level rise magnitudes. The quality of the forecast validation of the model is subject to a level of uncertainty itself. This is because the time period of the validation had low rainfall, with relatively few lake level rise events.

The model was shown to be limited by the assumption being made by the model that rain gauge rainfall is representative of the spatially average catchment rainfall. This is most often not the case and leads to errors in the model outputs. It may be possible to improve the predictive ability of the model by sourcing rainfall data more representative of the spatially average catchment rainfall. The model will also likely be improved by performing a recalibration using forecast data, this is highly recommended once more data becomes available.

While not perfect, as with any hydrological model, the model has shown to be able to reasonably forecast lake level changes in an operational situation, when considering the uncertainties associated with forecast rainfall and rain gauge data.

Acknowledgments

First and foremost, I must give thanks to my supervisor, Associate Professor Earl Bardsley, for providing me with the opportunity to carry out my research. Thank you so much for your guidance, support, and positive attitude when I needed it most. It has been an absolute honour to have been your student.

I would also like to thank Contact Energy for providing me with funding to carry out my research and in particular Malcolm Taylor, my liaison with Contact Energy, for approaching The University of Waikato with the idea for my project. Thank you for always making time for me, readily answering all my queries and providing me with the necessary data requirements. Also, thank you to the Contact Energy team down at the Clyde Dam for your hospitality when I came to visit.

I acknowledge The University of Waikato for awarding me with funding through a University of Waikato Masters Research Scholarship and also providing me with my own desk space on the beautiful campus grounds. Thank you to all the staff members and my fellow students within the Faculty of Science and Engineering for creating such a positive working environment, always having time for quick chat and coffee break. A special thanks to Cheryl Ward, the science librarian, for your eagerness to help with all my editing and referencing needs throughout my studies.

I extend my thanks to my family and friends for being so understanding of me being too busy to make many gatherings, getting me away from my desk, and always being there for me. Thank you to Katy and Andrew for keeping my belly full, with all your much-appreciated home cooked meals. And thanks to my good friends Samira, Hannah, Ashley, Sharnae and Yjosine, although you guys had no idea what I was talking about you were always there to listen to me babbling on about thesis work.

And finally, to my father, Graeme Waters, I cannot thank you enough for your support and encouragement throughout my studies. Not only did you convince me to return to study, which I'm forever grateful for, but you have also done everything in your power to make my time at university as stress-free as possible. Nothing you have done for me during this time has gone unnoticed and I will be forever grateful for it.

Table of Contents

List of Figures

Chapter 1 - Introduction

1.1 Introduction

Around 80% of New Zealand's electrical energy comes from renewable sources, with hydro-power generation a vital component of the country's renewable energy supply (Ministry of Business Innovation & Employment, 2018). The Clutha catchment is New Zealand's largest catchment, draining New Zealand's largest, by discharge, river the Clutha River situated in the Otago region of the South Island (Murray, 1975). Contact Energy operates two hydro-power stations along the Clutha River, the Clyde Dam and downstream the Roxburgh Dam (Fig. 2-1), together supplying around 10% of New Zealand's electrical energy.

The inflows into the hydro-power station's head-pond lakes, Lake Dunstan (above Clyde Dam) and Lake Roxburgh (above Roxburgh Dam) are significantly influenced by the outflows from three large lakes in the upper catchment area, Lake Wakatipu, Lake Wanaka and Lake Hāwea. There is a limited storage capacity in the hydro-scheme, with a small amount of seasonal controlled flow from Lake Hāwea, otherwise the hydro-scheme is predominately "run-of-river" (Taylor & Bardsley, 2015).

The nature of New Zealand's electricity market allows generators to make market offers up to 36 hours prior to generation. As there is limited storage capacity in the Clutha River hydro-scheme, it is essential for Contact Energy to be operating a short-term inflow forecast model with a reasonable degree of accuracy, to help quantify how much power can/will be generated to produce the market offers. The use of an inflow forecast model not only helps the station's operators make informative decisions regarding market offers, but also serves as a valuable tool for decision making concerning flood risk, power-production scheduling, management of water resources, spillway operation, dam safety and ensuring operational efficiency is maintained at all times (Collischonn *et al.*, 2005).

Contact Energy has identified possible improvement of the predictive power in their current Lake Dunstan reservoir inflow forecast model, which operates at the lead-time from 1 hour out to 48 hours. Over 80% of the inflow in Lake Dunstan is made up of the outflows from the upper catchment lakes, Lake Wanaka, Lake Wakatipu and Lake Hāwea. It is therefore possible to enhance the inflow forecasts by increasing the forecast accuracy of the forecast lake levels further up in the

catchment. A lake level forecast for Lake Hāwea is not required as its outflow is fully controlled.

1.2 Objectives

The purpose of this thesis is to improve the inflow forecasts into Lake Dunstan to aid operational efficiency of the Clutha power-scheme. This will be achieved through two objectives:

I. Develop an empirical lake level forecast model for the short-term lake level changes in Lake Wanaka and Lake Wakatipu, with lead-times out to 48 hours.
II. Perform an evaluation of the model operational performance. This will be done by using forecast rainfall as the model input thus providing a measure of the predictive uncertainty of the model when in operation after completion.

1.3 Thesis Outline

This thesis is organised by the following chapters, each on different components of the research:

Chapter 2 presents an overview of the Clutha catchment, including the local geography, hydrology, climate and snow effects. It also presents the locations of the rain gauges used in the model.

Chapter 3 reviews relevant literature on hydrological model development, and the problems associated with using rain gauge rainfall and forecast rainfall data as model inputs.

Chapter 4 details the development and structure of the empirical lake level forecast model, presenting the selecting parameters of the model when applied to Lakes Wanaka and Wakatipu.

Chapter 5 presents a visual inspection of the model calibrated fit for both Lakes Wanaka and Wakatipu. There is also an evaluation of the performance of the model when validated using rain gauge rainfall and recorded temperatures as model inputs.

Chapter 6 investigates the correlation between recorded rain gauge rainfall and forecast rainfall. The results are then used to evaluate the model performance as would be expected during operation. This evaluation is carried out using forecast temperature and rainfall as model inputs.

Chapter 7 presents conclusions and recommendations.

Chapter 2 - Study Area

2.1 Introduction

The catchments of Lakes Wanaka and Wakatipu are sub-catchments in the upper region of the Clutha catchment (Fig. 2-1). This chapter presents a brief overview of the Clutha catchment, detailing the regional geography, climate, snow and hydrology.

The Clutha catchment is New Zealand's largest catchment, spanning an area of 21,400 km^2 (Murray, 1975), and draining the Clutha River, with a mean annual flow of about 600 m^3s^{-1} at Balclutha, near the river mouth (Poyck *et al.*, 2011). The Clutha catchment is located in the Otago province of New Zealand's South Island. The catchment is situated south-east of the of the Southern Alps, a prominent mountain range. The Southern Alps extend 800 km along most of the western side of the South Island. Its watershed, the Main Divide, separates the western-draining catchments from the drier eastern-draining catchments.

The hydrology of the Clutha River in greatly influenced by the outflows of Lakes Wanaka and Wakatipu, along with a third large lake, Lake Hāwea. The lakes collectively make up around 75% of the Clutha flow at Balclutha. The headwaters of the three lakes border the eastern side of the Main Divide (Fig. 2-1). The lakes are therefore subject to the spill-over precipitation from the dominating north-westerly flows that create high rainfall on western side of the Main Divide (Chinn, 1979; Sinclair *et al.*, 1997).

2.2 Topography

Lakes Wanaka, Wakatipu and Hāwea, all lie within the alpine region of the catchment, with land elevations being mainly above 500 m. The elevations in the catchments of Lakes Wanaka and Wakatipu do not differ greatly (Table 2-1), with the Lake Wanaka catchment reaching a max elevation of 3,036 m and Lake Wakatipu reaching 2,819 m. The surface elevation of Lake Wakatipu is around 311 m, somewhat above Lake Wanaka's of 279 m (Murray, 1975).

Table 2-1: Elevation statistics for Lake Wanaka and Lake Wakatipu. Adapted from Murray (1975).

Elevation (m)	Lake Wanaka	Lake Wakatipu
Max (catchment)	3,036	2,819
Median (catchment)	1,356	1,274
Lake level	279	311

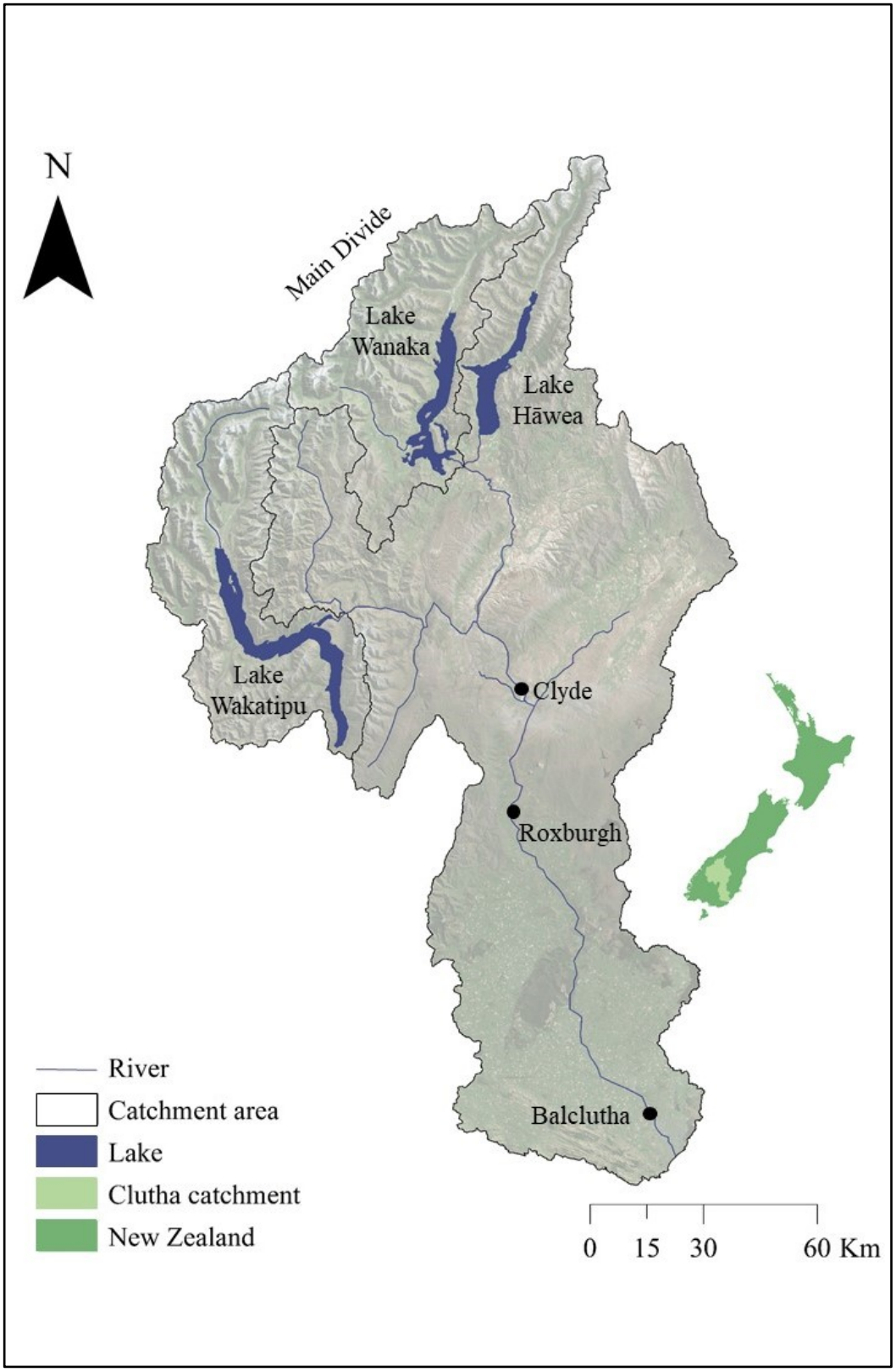

Figure 2-1: Main rivers, large lakes (with respective catchments) and selected place locations in the Clutha catchment. The insert shows the location of the Clutha catchment within New Zealand.

2.2.1 Climate

The local climate of the Clutha catchment is highly variable due to being significantly influenced by the Main Divide, which acts as a barrier for the predominant westerly airflows of the area (Fitzharhis, 1992).

2.2.2 Rainfall

The spatial distribution of precipitation in the upper Clutha catchment is typical of a mountainous terrain, with rainfall patterns being strongly influenced by the orographic effect. Moist airflows come primarily from the west and as the systems move landwards off the Tasman Sea, the airflows are forced to move up the western side the Southern Alps (Macara, 2015). This greatly increases the local precipitation there, which can exceed 10,000 mm per year.

As a result, the eastern side of the Southern Alps is subject to a rain shadow effect and receives considerably less precipitation. For the Clutha catchment, this causes a rainfall gradient, with greater than 4,000 mm per year in the high elevations bordering the Main Divide, then decreasing eastwards (Fig. 2-2). Annual rainfall can be as low as 400 mm per year within the inner basin (Fitzharhis, 1992), which is the driest location in New Zealand (Macara, 2015).

Table 2-2 lists the monthly normals for rainfall at locations around the upper Clutha catchment. Makarora, Queenstown and Wanaka, all near Lakes Wakatipu and Wanaka catchments, have evenly distributed rainfall throughout the seasons. Eastwards at Clyde the rainfall tends to be relatively higher during the summer months, mostly due to heavy rainfall events rather than more rain days during summer (Macara, 2015).

Table 2-2: Monthly rainfall normals in mm (a) and monthly % annual total rainfall (b) at selected locations in the Clutha catchment, for the period 1981-2010. Adapted from Macara (2015) .

Location		Jan	Feb	Mar	Apr	May	Jun	Jul	Aug	Sep	Oct	Nov	Dec
Clyde	a	51	41	33	34	32	33	24	24	26	36	35	49
	b	12	10	8	8	8	8	6	6	6	9	8	12
Makarora	a	197	134	194	175	202	228	185	217	232	241	190	251
	b	8	5	8	7	8	9	8	9	9	10	8	10
Wanaka	a	55	35	44	47	58	60	38	52	57	48	35	66
(airport)	b	9	6	7	8	10	10	6	9	10	8	6	11
Queenstown	a	64	48	53	56	72	72	49	69	67	66	68	76
(airport)	b	8	6	7	7	9	10	6	9	9	9	9	10

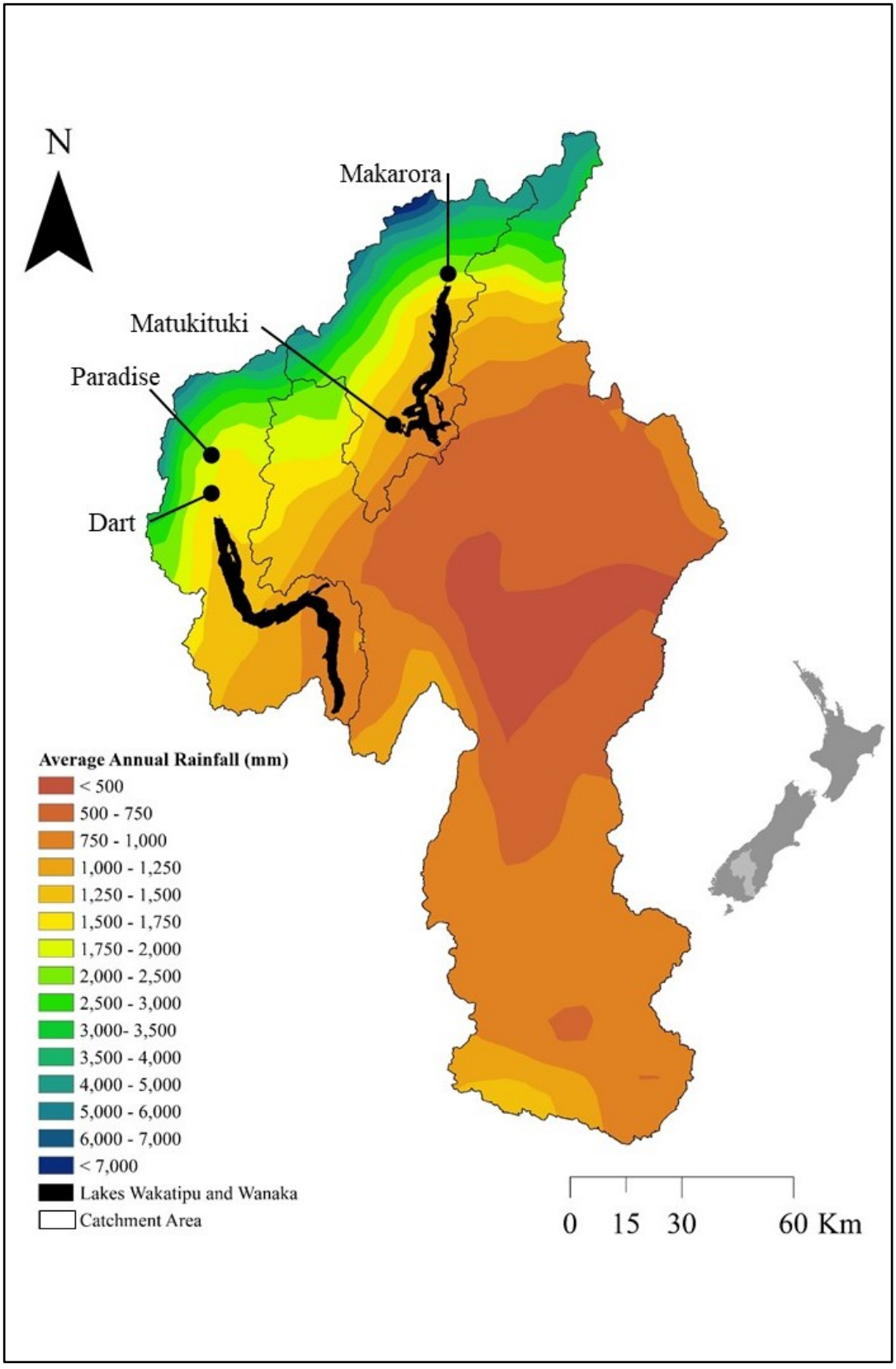

Figure 2-2: Average annual rainfall distribution across the Clutha catchment for the years 1972 – 2013. The map shows locations of the four rain gauge sites used within the study. Lake Hāwea is not shown. Data retrieved from Ministry for the Environment (2016).

2.2.3 Temperature

The Clutha catchment has a temperate climate with summer average daily maximum temperatures reaching between 18°C and 24°C and winter average daily minimum temperatures falling between -2°C and 3°C. This does not hold true for the higher elevations within the catchment, as the temperature drops with increasing elevation. Temperature in these higher regions tend to remain cool all year round, with glaciers and perennial snow present (Macara, 2015).

Table 2-3 shows the mean monthly temperature recorded at the Matukituki rain gauge site (Fig. 2-2), demonstrating the high seasonal variability of temperature within the area.

Table 2-3: Mean monthly air temperature (°C) for the period from 2006-2016 for Matukituki. Calculated from the data record provided by Contact Energy.

Location	Jan	Feb	Mar	Apr	May	Jun	Jul	Aug	Sep	Oct	Nov	Dec
Matukituki	17.1	16.9	14.3	10.9	7.3	3.8	3.2	5.9	9.0	11.5	13.8	16.4

2.3 Hydrology

The natural hydrology of the Clutha River has been altered by discharge control at Lake Hāwea, and construction of two hydroelectric dams. The upstream dam is the Clyde Dam, at Clyde, with the head-pond Lake Dunstan. Downstream from the Clyde Dam, Lake Roxburgh is the head-pond of the Roxburgh Dam, at Roxburgh.

The Clutha River begins as the natural outflow of Lake Wanaka, which is the greatest contributor to discharge further downstream. Just over 4 km downstream from the Wanaka outflow the Clutha River is met by a main tributary, the Hāwea River, sourced from the controlled outflow of Lake Hāwea. The river then flows southwards, collecting water from tributaries, including the Cardrona River and Lindis River, before flowing into Lake Dunstan, the man-made head-pond lake of the Clyde Dam.

The Kawerau River also flows into Lake Dunstan from the West, at the location where prior to the construction of the Clyde Dam was the natural confluence of the Clutha and Kawerau Rivers. The Kawerau River begins at the outflow of Lake Wakatipu and is met by a main tributary the Shotover River just downstream. The Kawerau River continues eastwards to Lake Dunstan, gaining water from tributaries including the Nevis and Arrow.

Lake Dunstan water discharges through the Clyde Dam flowing into Lake Roxburgh, which also gains water from the Manuherikia River. From the Roxburgh dam, the Clutha River flows south-east through the lower catchment area, discharging into the Pacific Ocean downstream from Balclutha (Fig. 2-1).

Lakes Wakatipu (293 km^2) and Lake Wanaka (192 km^2), are respectively New Zealand's third and fourth largest lakes by area. Both lakes have several inflowing tributaries, with the Dart and Rees Rivers the largest for Lake Wakatipu and the Makarora and Matukituki Rivers for Lake Wanaka. Although the rainfall at the Wanaka and Queenstown sites does not vary significantly throughout the seasons (Table 2-2) the inflows into the lakes vary considerably with season.

The lowest inflows into the Upper Clutha lakes occur during mid to late winter as the catchments' precipitation is stored as accumulated snow. The highest inflows usually occurring late spring/early summer due to snowmelt (Taylor & Bardsley, 2015). This seasonal variation is displayed in Figure 2-3 for the Dart River.

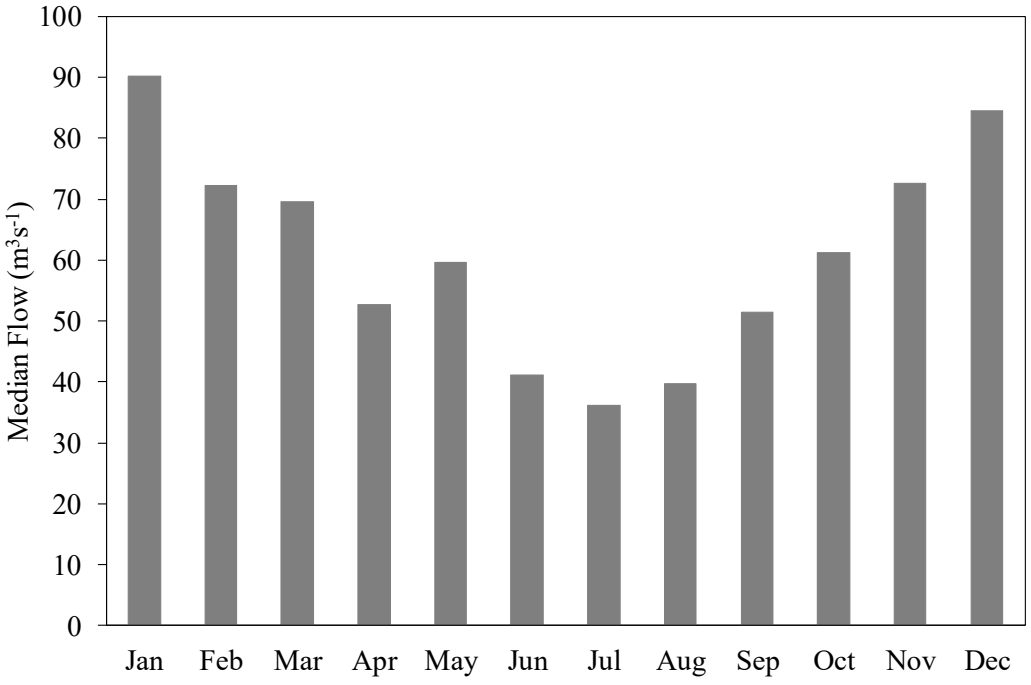

Figure 2-3: Median monthly flow for the Dart River, for the years 2006-2014. Data record provided by Contact Energy.

2.4 Lake Wakatipu

Lake Wakatipu has two notable characteristics. Firstly, the lake level is subject to a seiche which on average has a fundamental period of around 50 min and an average amplitude of around 0.10 m. The amplitude and timing of the seiche is highly influenced by weather patterns (Bottomley, 1955).

Secondly, the outflow rates of Lake Wakatipu under normal conditions are influenced by the modified outflow structure, redundant gates, and the characteristics of the Kawarau River. However, during times of high flow in the Shotover river, the outflow of Lake Wakatipu is reduced. This is because the Shotover River raises the stage level of the Kawarau River around 3 km downstream of the Wakatipu outflow and as a result the difference in elevation between Lake Wakatipu level and the stage level of the Kawarau river is reduced.

When this reduction in stage difference is large enough it reduces the outflow rate of Lake Wakatipu and on rare occasions can cause the Kawarau River to backflow into Lake Wakatipu (Webby & Waugh, 2006). This is further complicated by the high sedimentation rates of the Shotover River, also causing the stage difference to reduce. This effect is illustrated in Figure 2-4, showing the Lake Wakatipu outflow reducing during a period of high Shotover flow.

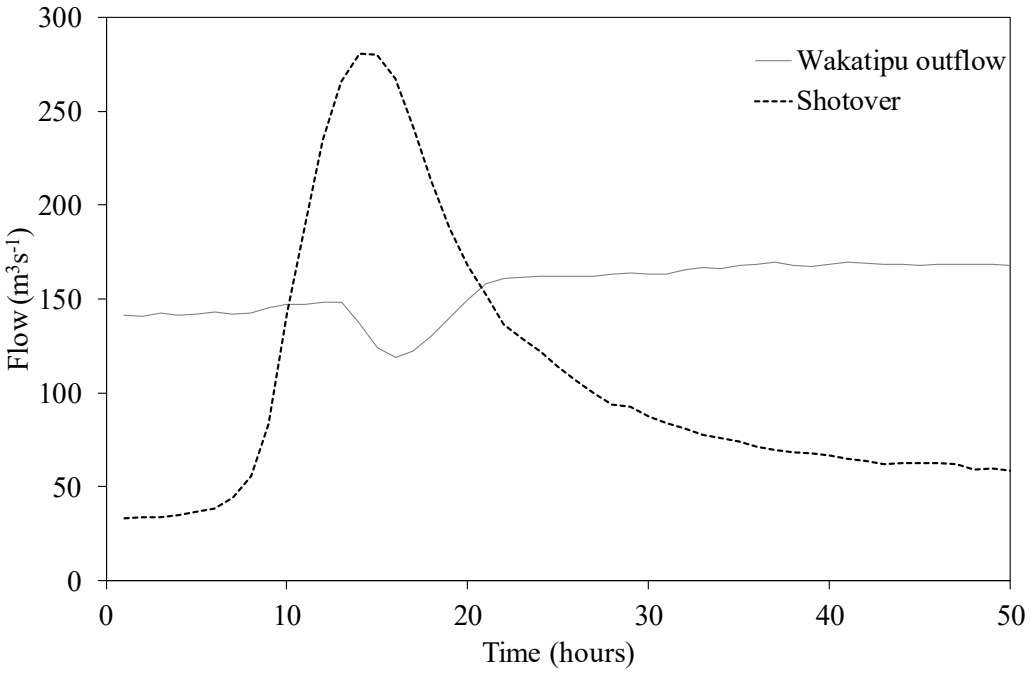

Figure 2-4: An example of an event occurring on 24nd June 2014 here the Lake Wakatipu outflow was reduced during a period of high Shotover flow.

2.5 Snow

Snowfall is common throughout the Clutha catchment, with substantial amounts falling in the alpine regions, where precipitation mainly falls as snow above the 3,000m elevation (Fitzharris, 1992). The catchment has large snowfields present from around late autumn through to early summer (Macara, 2015). The winter snowline is highly variable in the catchment. This is shown by Fitzharris and Garr

(1995), who developed a conceptual degree-day model (*SnowSim*) to calculate past variability in seasonal snow deposition and melt in the Southern Alps, which was validated on a restricted set of past snow observations. The model showed no seasonal trend in snow cover but indicated large interannual variability in the catchments.

In general, snow cover usually covers around 40% of the upper Clutha catchment area in winter, above around 1,000 m in the south and 1,300 m in the north. By the end of summer the snowline has usually retreated above 2,000 m, covering less than 5% of the upper catchment area (Fitzharhis, 1992).

Kerr (2013) applied a model to estimate the contribution of snowmelt to streamflow for the whole of the South Island, from 1981 – 2009. The model indicated snowmelt contributes just 13% of the mean annual inflows to Lakes Wakatipu and Hāwea, with only an 11% contribution to the mean annual inflows of Lake Wanaka. The model indicated that the Clutha at Roxburgh had a mean annual snow contribution of 12%.

2.6 Conclusion

The Clutha catchment is subject to high variability of hydroclimatic components, both spatially and temporally. The precipitation in the catchment declines strongly from west to east, due the orographic effects of the Southern Alps and the prevailing westerly wind patterns. Although the precipitation rates do not vary greatly throughout the year for the upper Clutha catchment, the streamflow's within the catchment vary greatly seasonally due to snow melt and snow accumulation. The winter snow inputs to the catchment are subject to significant interannual variability, but on all-year average provides around 12% of the annual inflow into the upper catchment lakes.

Chapter 3 - Literature Review

3.1 Introduction

Hydrological models have been around for a long time with the earliest widely-used model dating back over 160 years, a very basic model used simply to predict flood peaks for engineering purposes, such a bridge and culvert design (Beven, 2012). Since then hydrological modelling has rapidly evolved in parallel to our ever-increasing scientific knowledge and understanding of hydrological processes, the advancement of computing processing power allowing for the computation of complex model structures, and the expanding range of possible applications for the models (Beven, 2012; Todini, 2007). There are now countless models in use today with varying complexity, structure, application and forecasting abilities (Todini, 2011).

Many hydrological models are designed to increase the scientific knowledge and understanding of the hydrological processes occurring within the environment, however, they also have various practical uses outside of the scientific community, helping to solve the numerous hydrological problems the wider community experience (Kirchner, 2006). These problems include flood management, contamination, irrigation, water allocation, and the general operation of hydro-schemes and waste-water treatment plants (Beven, 2012; Gragne *et al.*, 2015b; Hosseini & Aqeel Ashraf, 2015; Mohssen & Goldsmith, 2011).

The objective of this thesis is to develop and evaluate an operational lake-level change forecast model, using a combination of rain gauge and forecast rainfall data. This chapter aims provide a context of where this thesis fits into the relevant literature, through the following two aims:

I. Give a brief discussion on hydrological model development and the current ideas and issues currently being considered within the literature.
II. Present an overview of the driving input into most hydrological models, rainfall data, focusing on rain gauge and forecast data.

3.2 Model Development

Although there is a vast amount of developed models available, with the majority of hydrologists being model users, many hydrologists are still tasked with developing a model (Beven, 2012). The leading motivation behind the continuation

of model development is to add more and more complexity to the models, although almost all scientific articles about the developed models conclude in same way stating the need for more data and computing power; a conclusion that has been common since the first use of computers in hydrological modelling (Sivakumar, 2008b). A common method of developing hydrological models is by improving on and modifying existing models (Perrin *et al.*, 2003), this has been done throughout hydrological modelling history. As is the case for one of the most famous hydrological models, the HBV model (Bergström & Forsman, 1973), which over the years has had numerous modifications continuously improving the structure (Lindström *et al.*, 1997; Mendez & Calvo-Valverde, 2016). However, many hydrologists still choose to develop a new model. When developing a new model there are typically three main stages from start to finish, first deciding upon the model structure, followed by calibration, and finally model evaluation (Wagener *et al.*, 2001), although model evaluation may lead to the reassessment the model structure, creating a looping model development process (Beven, 2012).

3.2.1 Model Structure

Deciding upon a model structure largely depends on the proposed application and need of the model (Wagener *et al.*, 2001), as time-consuming complex models may not be necessary for simple model requirements (Beven, 2012). It can be difficult to determine a model structure as there is no generalised hydrological theory which provides a way to simulate catchment behaviour (Perrin *et al.*, 2003). Due to this there is division among hydrologists over the necessary type of hydrological model structure, physical vs lumped. The first view is that hydrological models must place a high importance on representing the physical heterogeneity properties of the catchment, improving on the knowledge of the hydrological processes within the catchment, this type of modelling is referred to as physical modelling, also known as the upwards approach (Sivapalan *et al.*, 2003; Todini, 2011). The second view places high importance on finding the relationship between the model inputs and outputs, regardless of complex physical processes that occur, lumping them together in one or more transformation equations, this type of modelling is referred to as lumped modelling (Beven, 2012; Todini, 2011), also referred to as the downward approach (Sivapalan *et al.*, 2003).

Some hydrologists have further split lumped models into empirical (or metric) and conceptual, the empirical models take no account of the hydrological processes

within the catchment, ignoring the spatial variability in the rainfall-runoff relationship, simply transforming input data to output data (Kokkonen & Jakeman, 2001). The foundation of empirical models in hydrology was the development of the unit hydrograph theory by Sherman in 1932 (Beven, 2012; Kokkonen & Jakeman, 2001; Todini, 1988), which uses a time distribution to represent the various time delays of runoff from different parts of the catchment becoming one of the most widely used hydrograph modelling techniques in hydrological modelling (Beven, 2012). Using probability distribution functions to derive instantaneous unit hydrographs has been common throughout literature (Ghorbani *et al.*, 2017; Roy & Thomas, 2016). Bardsley (1983) suggested the use of the inverse Gaussian distribution as an alternative form for the instantaneous unit hydrograph over the more commonly used gamma distribution, as the inverse Gaussian distribution can describe some hydrographs with high peaks and long tails for which the gamma distribution would fail. A more recent approach to empirical modelling is the use of artificial neural networks (Dawson & Wilby, 2001).

Conceptual models sit between metric models and physical models, still lumping many hydrological processes together but with varying levels of conceptualism. Conceptualism is the degree to which a model structure can be related to catchment scale processes. This can be done by; simply splitting a catchment up into many sub catchments; splitting runoff into lagged subsurface runoff and quicker overland flows; or taking into account evaporation; all without taking in as much detail as a physical model (Kokkonen & Jakeman, 2001). The HBV model is an example of a conceptual model (Bergström & Forsman, 1973), dividing catchments into sub catchments, further dividing them into elevation zones and vegetation zones then applying a water balance equation (Devi *et al.*, 2015).

Physical models require large amounts of data and an understanding of the processes within a catchment, and therefore typically have large amounts of parameters and equations, which represent real processes (Devi *et al.*, 2015). Though many processes within catchments are well understood on catchment scales such as, interception loss, evaporation and infiltration in homogenous soils, the subsurface processes are still not well understood on small scales let alone catchment scales (Perrin *et al.*, 2003). The assumption is made during the development of physical models, that it is possible to upscale these small-scale processes (Freeze & Harlan, 1969). This limits the practicability of the models as

some processes are not applicable on large scale, leading to the argument that these models are technically no longer physically based (Beven, 2002b).

For researching the effects of land-use changes on streamflow within a given catchment and extrapolating that into the future where further land-use change may take place, it would be useful to use a physical model, which would consider the heterogeneity of the land in the catchment (Beven, 2012; Kirchner, 2006). However, in other applications where streamflow forecasting is required, the heterogeneity of the land may not be useful, bringing more potential pathways for error. Lumped models are likely to do better to fulfil the model flow forecasting purposes, with the advantage of using physical models having not yet been demonstrated (Perrin *et al.*, 2003).

Hydrological models can be further categorised as deterministic or stochastic models. Deterministic models produce one output from the set of input and parameter values, while stochastic models incorporate some form of the uncertainty into the model output values. This distinction is not always well defined as many models may add a stochastic error component to an output produced in a deterministic way or a model may use a probability distribution function within the model but produce output in a deterministic way (Beven, 2012).

3.2.2 Simplicity

Once a model structure is chosen the degree of complexity must be decided, this is an important step as too few will result in a model with limited flexibility and too many will result a decrease of the model robustness due to over-parametrisation (Perrin *et al.*, 2003). The complexity of a hydrological model is most often defined as the number of parameters a model has (Kokkonen & Jakeman, 2001; Perrin *et al.*, 2001; Perrin *et al.*, 2003). As scientific knowledge increases regarding the complexity of the hydrological processes, so does the complexity of many hydrologic models, this is particularly true for physical models (Perrin *et al.*, 2001; Sivakumar, 2008b). Sivakumar (2008b) stated "reading scientific articles... it does not seem possible (except in a few cases) to escape … more and more complex models, whether 'physically based' or 'black-box'". However, it has been argued throughout the literature, over whether this increasing complexity is further advancing hydrological models or simply increasing to the amount of possible errors, and therefore decreasing the operational practicability of the models (Beven,

2002a; Jakeman & Hornberger, 1993; Kirchner, 2006; Kokkonen & Jakeman, 2001; Perrin *et al.*, 2001; Sivakumar, 2008a).

Perrin *et al.* (2001) investigated the performance of 19 daily lumped models, all with three to nine parameters. It was shown that the optimal number of parameters for a model was three to five, with the more complex models being subject to over-parameterisation. Jakeman and Hornberger (1993) cover many studies where the reduction of parameters increased the predictive ability of the models, even a model with six parameters was discovered to be over-parametrised, they found in their own research that four parameters in a lumped model provided satisfactory results.

Nash and Sutcliffe (1970) suggests during model development the model should start off basic and only parameters that can be shown to increase the predictive ability and robustness of the model be added, as "each additional part of a model must substantially extend the range of application of the whole model". In cases where the model is already over-parameterised and simplicity is sought, Bardsley *et al.* (2015) suggests using the LASSO technique, the technique is able to select the parameters with high predictive power while eliminating unhelpful parameters.

3.2.3 Calibration

Model calibration is the process of adjusting parameter values within a model to give a better fit between observed and predicted values, to find the optimal parameter set, this can be done by either manual calibration or through algorithms which automatically calibrate the model (Beven, 2012).

At the most basic level, calibration of a model is carried out manually, done by visually inspecting the relationship between the model predictions and the observed data (Boyle *et al.*, 2000). Manual calibration can be extremely time consuming and requires an elevated level of user expertise with extensive knowledge of both the catchment and the model structure, however, manual calibration has the ability to produce excellent results (Beven, 2012). Automatic calibration on the other hand, which uses computing power is a quicker calibration method but may produce unacceptable results, especially in non-linear models (Duan *et al.*, 2004). This is because most algorithms find the local optimum parameter values in parameter space closest to the parameter starting values, which may not be the global optimum parameter values, especially in cases where irregularity exist in the parameter response surface. This may be avoided by starting the optimisation process several times with different starting values (Beven, 2012).

3.2.4 Validation

Model validation is the process of evaluating the model through the performance of the model abilities for prediction and/or simulation and can be assessed both qualitatively and quantitively (Biondi *et al.*, 2012). The split test is the most common method for selecting the validation time period, simply splitting up the data timeseries into a calibration period and smaller validation period (Klemeš, 1986). Qualitative techniques allow for subjective validation of the model through graphical techniques, the most common of which are time series and scatterplots allowing for identification of any patterns of error in the plots (Biondi *et al.*, 2012). Qualitative assessment of model performance is the most fundamental approach to assessing model performance, followed by quantitative assessment through performance metrics (Krause *et al.*, 2005). Performance metrics include the Nash-Sutcliffe Efficiency (NSE), mean absolute error (MAE) and root mean square error (RMSE) (Biondi *et al.*, 2012) and almost always tend to be biased towards larger errors in the model (Krause *et al.*, 2005).

The most common performance metric applied to hydrological models is the use of the NSE index (Jain & Sudheer, 2008), calculated by:

$$NSE = 1 - \frac{\sum_{t=1}^{N}(y_{obs}(t) - y_{sim}(t))^2}{\sum_{=1}^{N}(y_{obs}(t) - \bar{y}_{obs})^2} \quad (1)$$

where $y_{obs}(t)$ is the observed value at timestep t, $y_{sim}(t)$ is the simulated value and $\bar{y}_{obs}$ is the mean observed value over the length of simulation period N. The NSE can produce values from -∞ to 1, a value of 1 means the model has a perfect fit to the observed data, a value less than 0 means that the model of choice does worse than using the $\bar{y}_{obs}$ as the predictor (the benchmark model). However, the $\bar{y}_{obs}$ can be an extremely poor benchmark model in cases where there is strong seasonality in the timeseries, such a mountainous region, and can lead to the NSE generating a high value, which can easily be misinterpreted as a good model performance (Schaefli & Gupta, 2007). For example, Schaefli *et al.* (2005) ran a simple model in a high mountainous catchment using the historic calendar day mean as the model predictor and produced an NSE value of 0.85, when using the $\bar{y}_{obs}$ as the bench mark model.

Bardsley (2015) showed that using the current discharge as a bench mark model for evaluating a flood forecast model applied to the Leith River, Dunedin, New Zealand resulted in an NSE value of -0.44 in contrast to an NSE value of 0.71 when the

$\bar{y}_{obs}$was used as the benchmark model. This highlights the need for selecting a suitable benchmark model for model evaluation.

3.2.5 Uncertainty

Addressing the uncertainty of a model is an important part of model evaluation, however there is confusion within the literature on the difference between validation uncertainty and predictive uncertainty. Validation uncertainty is the evaluation of how well the model can mimic the observed values, this will highlight areas where the model may be able to be altered to improve the model structure and predictive uncertainty. Predictive uncertainty of a model is the uncertainty of the model's output, when the predicted value has not yet been observed (Todini, 2011). It is the predictive uncertainty that is important for flood management and hydro-schemes, as the operator must always be aware of this value as it is readily incorporated into decision making processes (Beven, 2012). Adaptive algorithms are often applied to real-time forecasting, continuously attempting to reduce model predictive uncertainty through adaptive gain parameters (Lees *et al.*, 1994). Updating algorithms may be applied to existing models, as shown by Gragne *et al.* (2015a) when they developed a model for continuous updating of the error for a reservoir inflow model, the model was an extension onto an existing modelling framework, which did not require modifying the model.

Furthermore, model uncertainty can also be classified into epistemic uncertainty and natural uncertainty (Merz & Thieken, 2005). The first type of uncertainty is epistemic uncertainty, which is caused from lack of knowledge (Renard *et al.*, 2010). In hydrologic models, lack of knowledge may come from our limited ability to take measurements, to understand the catchment and to describe the catchment (Merz & Thieken, 2005). In principle epistemic uncertainty may therefore be reduced by increasing our knowledge, however, this may be at a cost to time, money and resources (Beven, 2013). Natural uncertainties on the other hand are uncertainties considered to be non-reducible and stems from the variability of inputs over time, such as the amount of rainfall falling from year to year (Merz & Thieken, 2005).

Beven (2013) argues that epistemic uncertainties need to be considered and distinguished from natural uncertainties and that it is not acceptable to lump them together. Lumping uncertainties may mask important information of the model (Merz & Thieken, 2005), not allowing the model user to distinguish between the unknown and the accepted uncertainty. However, it is noted that separating

uncertainties is proving to be difficult, with no clear boundary between epistemic uncertainty and natural uncertainty. For example, the variability of rainfall annually may to some degree be explained by decadal weather patterns, therefore the line gets blurred as to if the variability is due to the lack of knowledge of weather patterns (epistemic uncertainty) or the natural variability (Beven, 2013).

3.3 Rainfall

Rainfall is highly variable in both space and time, making the measurement of rainfall difficult (Krajewski *et al.*, 2003), yet the accuracy of rainfall as an input into rainfall-runoff models is fundamental for adequate performance of the model (Wang *et al.*, 2009). For lumped models, which treat the catchment as one unit, the rainfall input is a spatial averaged value, adding uncertainty to the model as it is well known rainfall distribution is uneven over catchments (Li *et al.*, 2017). The error in rainfall data transfers into uncertainty in rainfall-runoff models' output, which has been well studied (Duncan *et al.*, 1993; McMillan *et al.*, 2011; Sun *et al.*, 2000), and makes it difficult for identifying the sources of error in a rainfall-runoff model, recognised as one of the major problems within the subject (Kuczera *et al.*, 2006). Rainfall is often considered the largest source of error in rainfall-runoff modelling (Kuczera *et al.*, 2006; McMillan *et al.*, 2011), and therefore recognition of the rainfall error is required for model assessment.

3.3.1 Rain Gauge Data

Rainfall-runoff modelling is heavily reliant on the records of rain gauges (Beven, 2012) and when using rain gauge data as the rainfall input into lumped hydrological models it is required that the rain gauges to be highly correlated to the mean areal precipitation occurring in the catchment (Duncan *et al.*, 1993). The spatial correlation of rain gauge data increases with averaging time (Villarini *et al.*, 2008). Villarini *et al.* (2008) performed a detailed study of rain gauge spatial and temporal correlation in a catchment area of 135 km^2, in the Brue catchment, England, using 50 rain gauges. This led to the suggestion that for accurate estimation of areal rainfall within 20% of its true values, for an area of 200 km^2, over 25, close to 25, 15, and 4 rain gauges required at the temporal resolution of 15 min, hourly, 3 hourly, and 24 hourly, respectively. The temporal resolution of rainfall required for hydrological modelling depends on the size and shape of the hydrograph (Aronica *et al.*, 2005), it is recommended that the time resolution of the rainfall should be

enough to be able to divide a rising limb into three time steps or more (Schilling, 1991).

Dong *et al.* (2005) investigated the appropriate spatial sampling of rainfall through rain gauges, with a temporal resolution of six hours, as use for an input into the spatially lumped HBV model for improving flow simulation in a large catchment area of 12 209 km^2 upstream of Yuxiakou, China. The results showed that the correlation coefficient between the mean areal rainfall and the number of rain gauges increased hyperbolically, levelling off at the critical number of rain gauges required, which they found to be five within the study area. The effect transferred through to the quantitative performance of the model, with the model performance increasing up to five rain gauges and levelling off thereafter. The top performing combination of five rain gauges for the study were also mostly located in areas of high elevation subjected to strong orographic rainfall.

3.3.2 Forecast Rainfall

Rainfall models take advantage of the increasing accuracy of rainfall forecasts, combining the forecast rainfall with real-time rainfall data improving streamflow forecasts (Cuo *et al.*, 2011) by extending the lead-time beyond the concentration time of the catchments (Cloke & Pappenberger, 2009). The introduction of rainfall forecasts significantly increases the uncertainty of hydrological models (Kobold, 2005), with some modellers arguing the accuracy of rainfall forecast still needing to be improved for reliable model predictions (Habets *et al.*, 2004). Other modellers argue using rainfall forecasts to extend stream-flow forecast lead-time is a valuable resource to improve decision making regarding water resource management, hydro-power operations and flood protection schemes (Collischonn *et al.*, 2005).

Habets *et al.* (2004) studied the benefit of using precipitation forecasts for prediction of streamflow, in the Rhone basin, France. They found river flows were predicted poorly using precipitation forecasts at a lead-time of 24 hours and even worse at 72 hours, as the forecast precipitations forecast skill reduced significantly during high rainfall events. However, they did note the precipitation forecasts were able to predict the occurrence of rain reasonably well.

Li *et al.* (2017) developed a streamflow forecast model to the Liujiang River basin, China, utilising rainfall forecast for use in a model calibrated on rain gauge data. They found the model performed reasonably well with the forecast data pre-recalibration, the results significantly improved once recalibration of the model was

undertaken using the forecast data. While the forecast skill still decreased with lead-time, the improvement of the forecast skill increased with increasing lead-time.

Rainfall-runoff models using rainfall forecasts are increasingly moving towards ensemble forecasts, which provide a range of possible future rainfalls, moving away from the deterministic forecast which produce one value (Cloke & Pappenberger, 2009). This adds value to operational systems as ensemble forecasts provide clear probabilities of the occurrence of rainfall events (Roulin & Vannitsem, 2005).

3.4 Conclusion

This chapter has presented an overview of the current state of hydrological modelling and the potential error they may encounter originating from the rainfall input data. There is a current trend to create more and more complex models, but the usefulness of such models is being questioned as they introduce several sources of error into the model and reduce the operational practicability. The choice of rainfall data in the model can greatly affect the performance of the model, rain gauge data must be spatially representative of the catchment area and the quality of forecast rainfall data can significantly affect the predictive uncertainty of the model.

Chapter 4 - Model Development

4.1 Introduction

This chapter covers the development and structure of the lake level forecast model applied to Lakes Wanaka and Wakatipu. The aim of the model is to seek to predict coming lake level changes as closely as possible. The aim is simply to have as high predictive power as possible for operational purposes, so the approach taken for model design is empirical matching to lake level changes using a small number of independent variables.

The model was developed to forecast future lake levels for every hour following current time, extending into the future as far as 48 hours. Forecasting future lake levels for any lake can be expressed generally as:

$$L_t = L_{t_0} + \Delta L_t \quad (2)$$

where L is forecast lake level at time t measured from current time t_0 and ΔL_t is the forecast change in lake level.

Rather than express model results as predicted lake level, the predicted lake level change ΔL is the focus of this thesis. The use of ΔL is preferred because its sign conveniently indicates whether the lake level is forecast to rise or fall. The equation used for predicting the lake level change in this model is expressed as:

$$\Delta L_t = I_t + D_t \quad (3)$$

where D_t is the predicted lake level recession component to some time t and I_t is any predicted lake rise increment component as a result of recent rainfall.

4.2 Lake Level Recession

The lake level recession component of the model predicts by how much the lake level will have receded by at time t, based on the gradient of a plot of a long-term record of lake recession rate as a function of lake level.

The first step for analysing lake level recession rates was selecting twenty time-periods of observed lake level recessions with minimal inflow events in the respective periods. These recessions were selected independent of the time of year and they collectively extend over a wide range of lake levels.

Next the lake level recession rates over a 48 hour period for various lake levels were plotted (Fig. 4-1 and 4-2), being the maximum extent of the forecast time. These plots show a 48 hour interval is a sufficient time interval for use in the gradient plots.

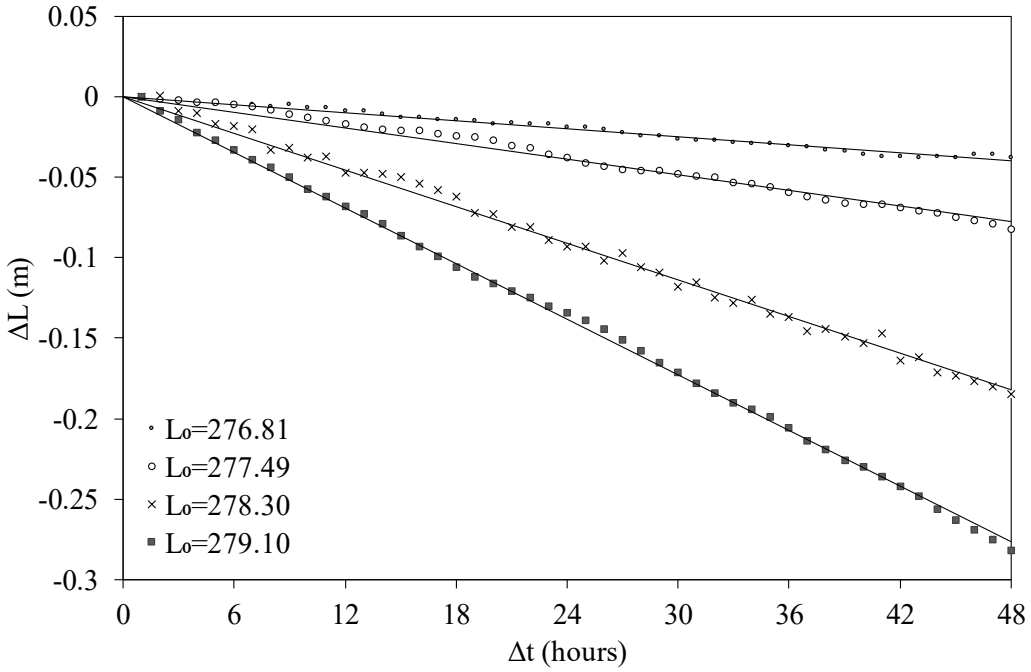

Figure 4-1: 48-hour linear declines in lake level for Lake Wanaka, for four different starting lake levels, L_0.

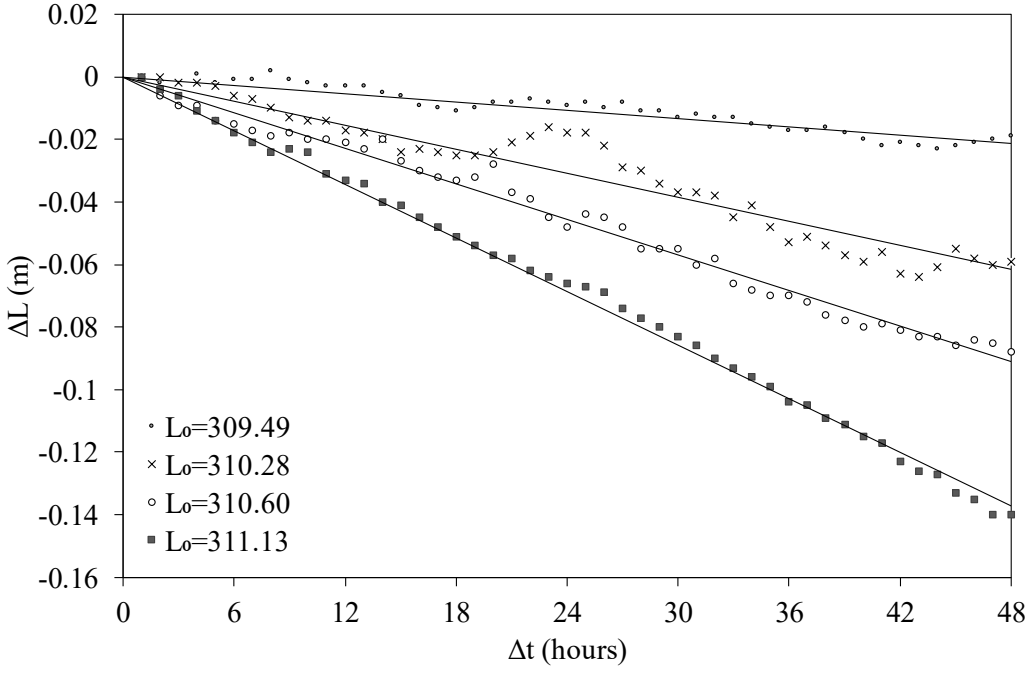

Figure 4-2: 48-hour linear declines in lake level for Lake Wakatipu, for four different starting lake levels, L_0. The small variation in the decline for $L_0 = 310.28$ is a common characteristic of Lake Wakatipu recessions.

Plots of L_0 against $\frac{\Delta L}{\Delta t}$ are shown in Figure 4-3 and 4-4, with fitted quadratic expressions of the type:

$$\frac{\Delta L}{\Delta t} = aL_0{}^2 + bL_0 + c \quad (4)$$

where a, b and c are the parameters of a quadratic regression model for each lake. The lake level recession D_t at time t, is then given by:

$$D_t = \left(\frac{\Delta L}{\Delta t}\right) t \quad (5)$$

The method is a simple way to calculate lake recession, with the following two assumptions being made; evaporation is negligible over a 48 hour period; variations in lake inflows during recession periods can be neglected, with lake level recessions being dominated by the outflow rate. However, the latter of two will not hold for high lake level recessions as the inflows may significantly influence on lake levels.

Lake Wanaka and Lake Wakatipu both experience noisy lake level recessions, due to small variations in the inflows and lake seiches. For Lake Wanaka the noise is not significant (Fig. 4-1) in comparison to the noise experienced in Lake Wakatipu (Fig. 4-2). The lake level in Lake Wakatipu can fluctuate substantially because of the lake's seiche, during periods of low lake level recession rates, the seiche amplitude may be larger than the recession rate causing the lake level to increase between two timesteps over 48. The is apparent in Figure 4-4, where a few data points are situated above zero on the y-axis.

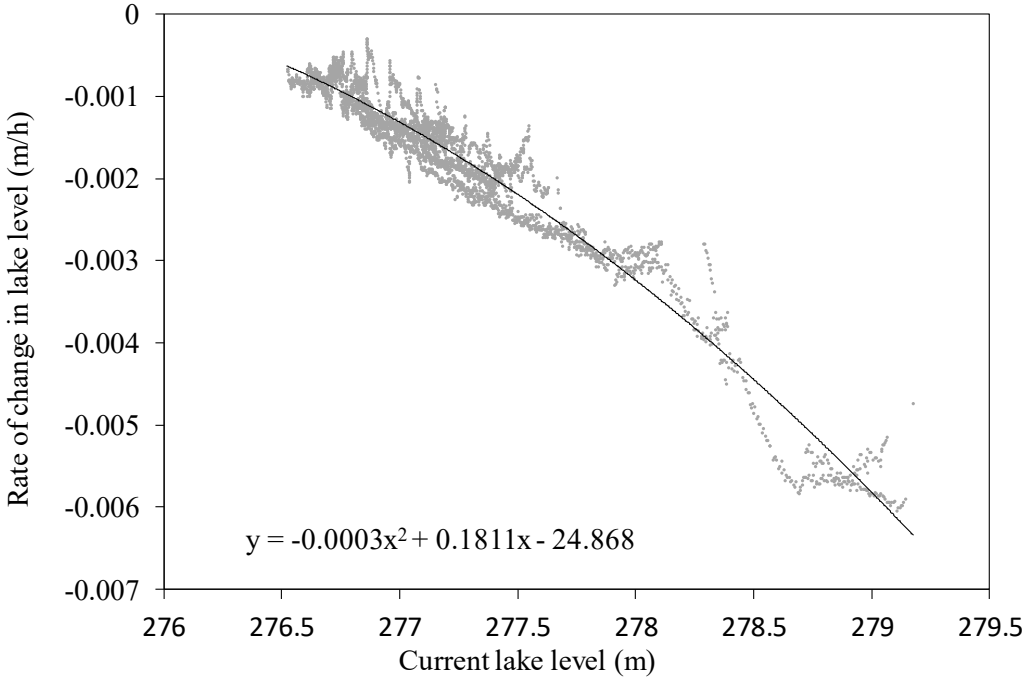

Figure 4-3: Recession plot showing the rate of decline in lake level against current lake level, for Lake Wanaka, for twenty time-periods with minimal inflow events. The data is fitted with a quadratic regression model.

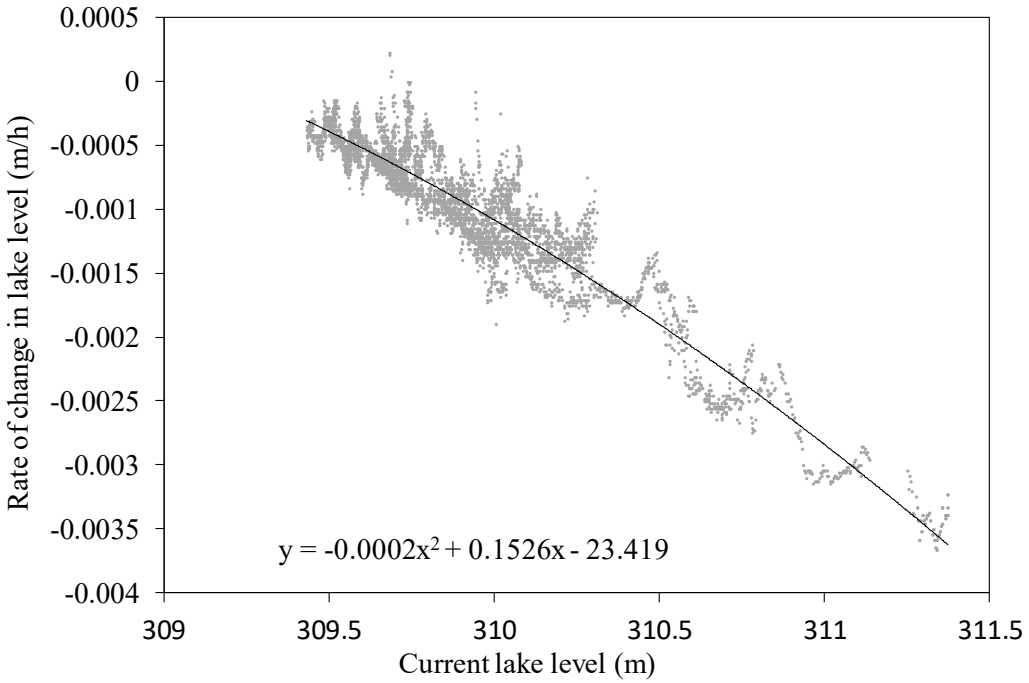

Figure 4-4: Recession plot showing the rate of decline in lake level against current lake level, for Lake Wakatipu, for twenty time-periods with minimal inflow events. The data is fitted with a quadratic regression model.

4.3 Lake Level and Inflow

The model lake level change increment from inflow predicts how much the lake level will rise by at time *t*, due to recent rainfall events increasing lake inflows. The inverse Gaussian distribution was selected to represent the form of the time distribution of lake inflows from a given rainfall event (section 4.3.2). Air temperature was used as a proxy for separating precipitation into snow accumulation and rainfall contributing to lake inflows (section 4.3.3) and a bias correction was added account for the models' underprediction of larger lake level rises (section 4.3.4).

During the development of the lake level inflow part of the model, the Excel Solver was sufficient for calibration, minimising the objective function:

$$\mathrm{AD} = \sum_{t=1}^{n} \left| \Delta L_t - \widehat{\Delta L}_t \right| \tag{6}$$

which is the sum of absolute deviations AD between the observed lake level changes ΔL_t and the predicted lake level changes $\widehat{\Delta L}_t$.

Absolute deviations were chosen to fit the data rather than other more common hydrological objective functions such as the NSE index and root mean squared error because these measures are weighted towards the larger differences between observed and predicted as a consequence of squaring residuals (Krause *et al.*, 2005). The developed model is to be used for operational purposes rather than flood forecasting, therefore, all changes in lake levels are of equal interest.

The lake inflow at each timestep is modelled in length dimension (metres) to directly represent the lake level change as a consequence of an inflow event, referred to as the total lake level rise hydrograph. To calculate the total lake level change I_t from an inflow event at time *t*, the total lake level rise hydrograph ordinates B_t are summed:

$$I_t = \sum_{i=1}^{t} B_i \tag{7}$$

where *i* is each of the timesteps forward of t_0 to time *t*.

4.3.1 Rainfall Data for Model Input

Preliminary results showed the most suitable rain gauges to use for Lake Wanaka lake level change forecasting were Matukituki (R_1) and Makarora (R_2), and for Lake Wakatipu, Dart (R_1) and Paradise (R_2), the location of these sites are shown in Figure 2-2. A weighting of the respective two rain gauges is used as the rainfall input into the model. The rainfall selected weighting values ω were obtained by finding the highest correlation between ΔL_{48} and the rainfall cumulation over the past 48 hours, for different weighting values ω within the 0,1 range (Fig. 4-5). A reinspection of Figure 4-5 indicates the use of Matukituki rain gauge was unnecessary and Makarora alone would have been sufficient for the model input.

Rainfall occurring after t_0 is forecast rainfall (R_f) and is scaled to match the average depth of the rainfall calculated using rain gauges (*see chapter 6*). For a given lake, the model rainfall input *P,* is obtained as:

$$P = \begin{cases} \omega . R_1 + (1-\omega) . R_2, & t \leq 0 \\ R_f . \omega_f, & t > 0 \end{cases} \quad (8)$$

Unfortunately, forecast rainfall was not available for calibration so instead hindcast validation has to be employed, with actual rain gauge data values used for "forecast" rainfall at times forward of t_0.

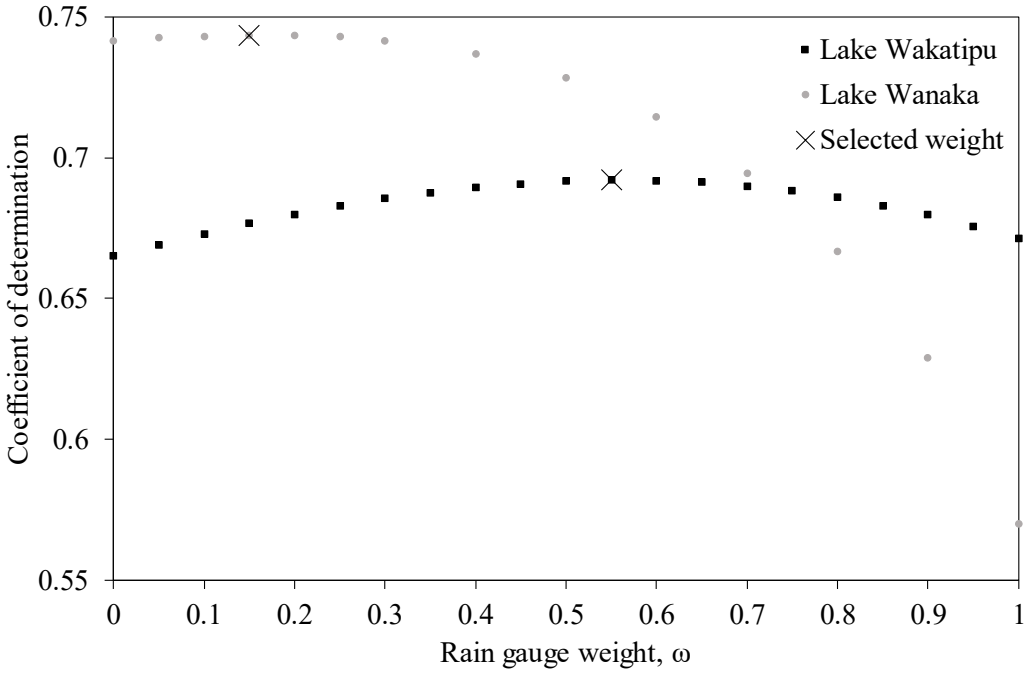

Figure 4-5: The coefficient of determination for the relationship between lake level changes and weighted rainfall plotted against different rain gauge weights. R_1 was given the weight ω, and R_2 given the weight 1 – ω. The highest R^2 value and chosen weights for the rain gauges are marked with ×.

4.3.2 Inverse Gaussian distribution

The inverse Gaussian distribution is a family of continuous probability density functions defined over the positive domain, with origin at zero for the two-parameter form which can be parameterised (Tweedie, 1957):

$$f(x;\mu,\Phi) = \left[\frac{\mu\Phi}{2\pi x^3}\right]^{\frac{1}{2}} \exp\left\{-\frac{\Phi x}{2\mu} + \Phi - \frac{\mu\Phi}{2x}\right\} \qquad (9)$$

$$x > 0, \Phi > 0, \mu > 0$$

where μ is the distribution mean and Φ is a shape parameter. As Φ increases, the distribution tends towards the normal distribution (Figure 4-6).

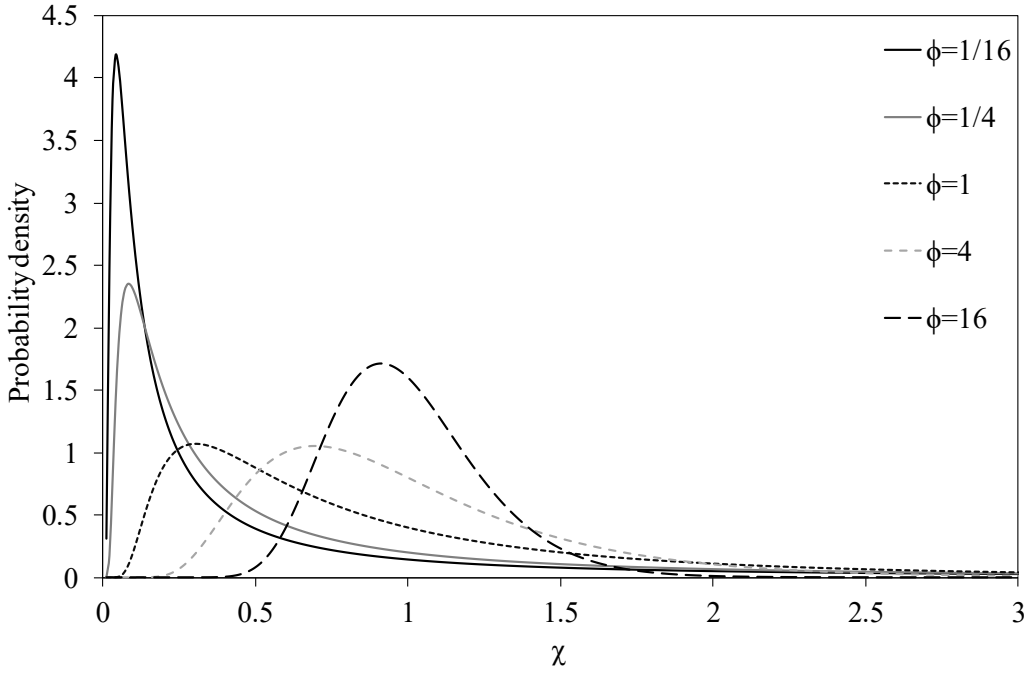

Figure 4-6: Comparison of five inverse Gaussian distribution forms for various shape parameter values (μ =1).

The inverse Gaussian distribution provides a range of hydrograph-like forms to estimate the time distribution of a lake level rise in the model from a single rainfall event, with χ representing the time from the rainfall event, and the probability density being proportional to lake level rise at subsequent times. The inverse Gaussian distribution was incorporated into the model as:

$$g_i = m.\left[\frac{\mu\Phi}{2\pi(i-0.5)^3}\right]^{\frac{1}{2}} \exp\left\{-\frac{\Phi(i-0.5)}{2\mu} + \Phi - \frac{\mu\Phi}{2(i-0.5)}\right\} \qquad (10)$$

where g_i is an individual lake level rise hydrograph ordinate in metres per millimetre of effective rainfall, from a rainfall event occurring i hours prior and m

being a multiplier parameter, which converts the inverse Gaussian probability density into lake level rise. A combination of Excel Solver and manual adjustment were used to estimate the parameter values for the inverse Gaussian forms used within the model (Fig. 4-7).

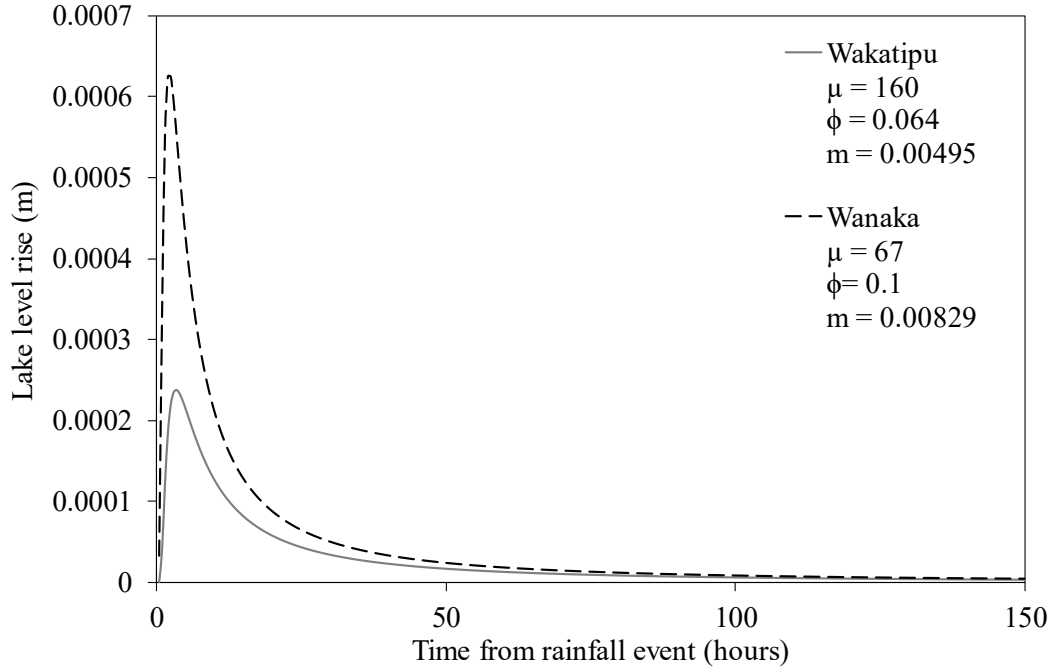

Figure 4-7: The calibrated individual lake level rise hydrograph forms for Lakes Wanaka and Wakatipu, estimating hourly lake level rises following 1mm of effective rainfall.

At any given time *t* the total lake level rise hydrograph is due to the cumulation of individual lake level rise hydrographs, one for each previous rainfall event. Calculation of the total lake level rise hydrograph at the time *t*, is done by taking the summation of the individual lake level rise hydrograph ordinates at time t, from the previous 300 timesteps of possible rainfall events:

$$G_t = \sum_{i=1}^{300} g_i p_{t-i+1} \tag{11}$$

where G_t is the total lake level rise hydrograph ordinate, at time *t*, and p is the effective rainfall at each of the previous 300 timesteps prior to t, many p values will be zero not contributing to lake level rise. This is essentially the same method used to calculate direct runoff hydrograph from multiple instantaneous unit hydrographs (Chow *et al.*, 1988).

4.3.3 Effective Rainfall

The percentage of rainfall contributing to lake level rise, here referred to as the rain proportion α, changes throughout the year due to snow accumulation. The rainfall proportion is calculated using two threshold mean temperatures T_{max} and T_{min}. When the mean catchment temperature of the past 24 hours T, is within the threshold range the rainfall proportion gradually changes over the following linear transition, using the Quick and Pipes (1977) equation:

$$\alpha = \begin{cases} 0, & T < T_{min} \\ \dfrac{T - T_{min}}{T_{max} - T_{min}}, & T_{min} \leq T \leq T_{max} \\ 1, & T > T_{max} \end{cases} \quad (12)$$

The parameters T_{max} and T_{min} were calibrated using both manual adjustment and Excel Solver (Table 4-1). Figure 4-8 shows the linear transition of rainfall proportion as a function of mean temperature. The effective rainfall, p, is calculated by:

$$p = \alpha P \quad (13)$$

where P is the rainfall input.

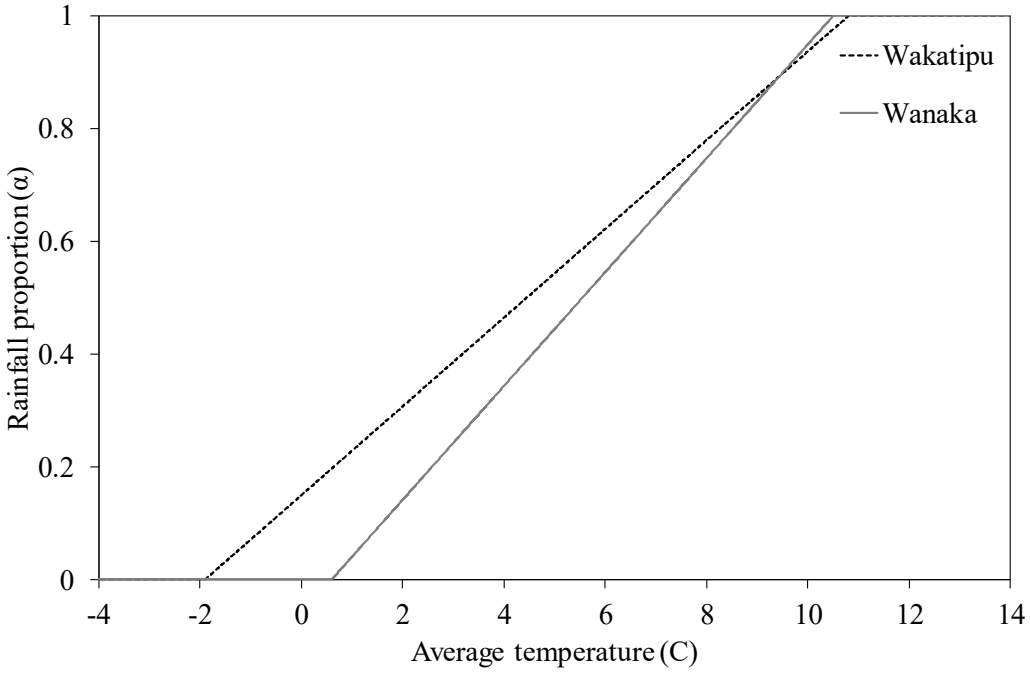

Figure 4-8: The rainfall proportion as function of the average temperature over the past 24 hours, for Lakes Wanaka and Wakatipu. When average temperature is outside of the range T_{min} (0.6°C for Lake Wanaka and -1.9°C for Lake Wakatipu) to T_{max} (10.5°C for Lake Wanaka and 10.8°C for Lake Wakatipu) rainfall proportion is equal to 1 or 0.

4.3.4 Bias Correction

The preliminary results of the model showed increasing under-prediction for the larger lake level rises. This was offset by running the G_t values through a quadratic transformation, essentially increasing the predicted higher total lake level rise hydrograph ordinates:

$$B_t = \beta {G_t}^2 + \Upsilon G_t \quad (14)$$

where B_t is the adjusted total lake level rise hydrograph ordinates, and β and Υ are the parameters of the quadratic equation. Figure 4-9 shows the adjusted total lake level rise hydrograph compared to the initial total lake level rise hydrograph predictions of the model, for a section of the calibrated data for Lake Wakatipu.

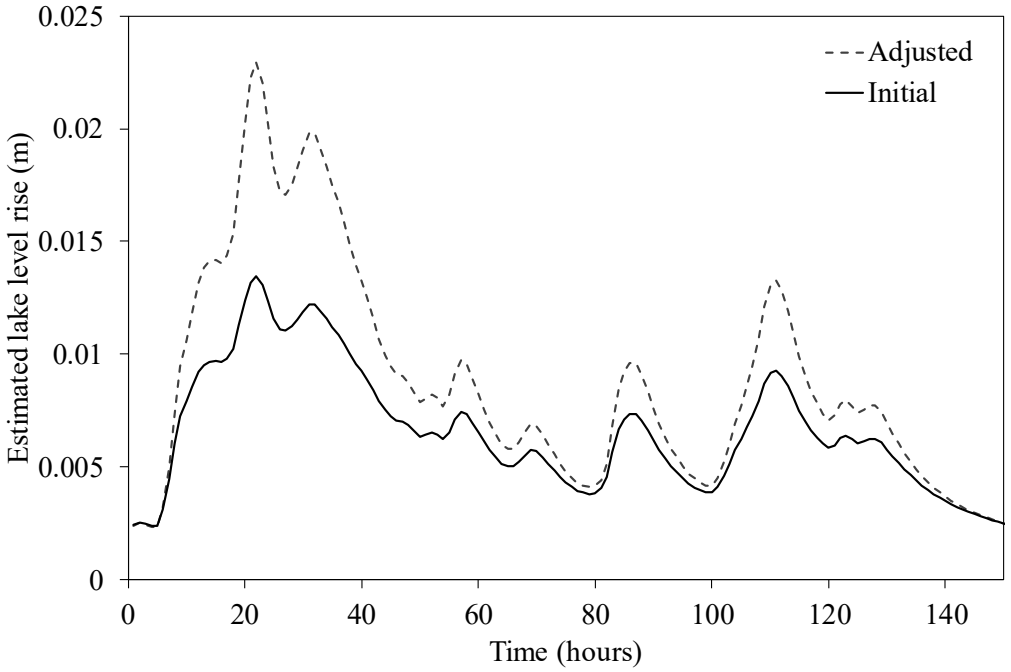

Figure 4-9: A section of the calibrated Lake Wakatipu data, showing the initial total lake level rise hydrograph prior to the quadratic transformation and the total lake level rise hydrograph.

4.4 Discussion

An empirical lumped model has been developed for application to Lakes Wanaka and Wakatipu, estimating the lake level changes using current lake level, precipitation and temperature data. The model estimates lake level change by adding the estimated lake level recession and the estimated lake level rise due to recent rainfall (Eq. (3). The estimated lake level recession is calculated as a function of current lake level using Eq. 4, then multiplied by the forecast lead-time (Eq. 5).

The estimated lake level rise from inflow events is calculated through multiple equations. The first step for the lake rise estimation is the calculation of the rainfall input P. For timesteps prior or equal to t_0, P is derived from rain gauge data and for timesteps forward of t_0, P is derived from forecast rainfall (Eq. 8). The proportion of rainfall contributing to the lake inflow is calculated using a linear transition between two temperature thresholds, parameters T_{max} and T_{min} (Eq. 12). The effective rainfall is then calculated using the rainfall proportion and the input rainfall (Eq. 13).

The time distribution of lake level from an event of 1mm of effective rainfall is calculated using the inverse Gaussian distribution, with a parameter m converting the probability density into lake level in metres per millimetre of effective rainfall, producing the individual lake level rise hydrograph form (Eq. 10). Summation of the individual lake level rise hydrograph ordinates at time t from the previous 300 timesteps gives the estimate the total lake level rise hydrograph ordinate at time t (Eq. 11). The total lake level rise hydrograph is then adjusted through a quadratic transformation (Eq. 14). Total lake level rise I_t at time t is then calculated by the summation of the total lake level rise hydrograph ordinates at each timestep after the current time t_0 up to time, t (Eq. 7).

The selected values for the respective parameters mentioned throughout for when the model is applied to Lakes Wanaka and Wakatipu are listed in Table 4-4.

Table 4-1: The parameters for the lake level change model for Lakes Wanaka and Wakatipu.

	Parameter	Units	Lake Wanaka	Lake Wakatipu
Lake Level Recession	α	-	-0.0003	-0.0002
	b	-	0.1811	0.1526
	c	-	-24.87	-23.42
Rainfall Weights	ω_f	-	0.57	0.64
	ω	-	0.15	0.55
Multiplier	m	$m.mm^{-1}$	0.00829	0.00495
Inverse Gaussian	ϕ	-	0.10	0.064
	μ	hours	67	160
Rainfall Proportion	T_{MAX}	C°	10.50	10.80
	T_{MIN}	C°	0.60	-1.90
Bias Correction	β	-	22.9571	65.2710
	Υ	-	0.8424	0.8296

4.5 Conclusion

The structure of the developed model has been described throughout this chapter. The model was calibrated using both Excel Solver and manual adjustment to estimate the selected parameter values. The model uses a quadratic function to predict lake level recession and estimates total lake level rise hydrographs using an inverse Gaussian distribution. A bias-correction is added to the model through a quadradic transformation of the total lake level rise hydrograph.

Chapter 5 - Calibration and Hindcast Validation

5.1 Introduction

This chapter describes and discusses the results of the calibration and hindcast validation of the developed lake level change model. The word "hindcast" is used to refer to this validation as the rainfall and temperature data input for timesteps forward of t_0 were recorded data, as a forecast dataset was not then available. A second validation of the model was later carried out once forecast data became available and is differentiated as the "forecast" validation (*Chapter 6*).

Although the completed model will be operated using forecast input data it is still useful to investigate how the model performs using the recorded rain gauge and temperature data. This is because the model was developed and calibrated using recorded data, so serves as a basis to determine the error increment introduced later with forecast data as input.

The calibration of the respective models for the two lakes was carried out for 2006 through to 2013 and the hindcast validation was for the years 2015 and 2016. The year 2014 was not used as most of the temperature record for that year was missing from the dataset.

For many of the plots throughout this chapter and Chapter 6, the results from only the observed and estimated change in lake level at a 48 hour lead-time have been presented. This is due to two main reasons, firstly the 48 hour lead-time is the furthest lead-time away from t_0 and will therefore, on average, have the largest change in lake level leading to the largest residual error. Secondly, the 48 hour lead-time has the highest signal-to-noise ratio for the observed change in lake level. This makes the plots clearer to visually inspect, buffering out the small lake level changes resulting from lake seiches and diurnal inflow variations from snowmelt.

It is noted again that the 48 hour lead-time lake level changes are referenced against current lake level, i.e., the difference between current lake level and the lake level 48 hours on. Thus, negative values denote actual and anticipated lake level decline and vice versa.

In calculating NSE values, current lake level was used as the base model for calculation purposes. As discussed in Chapter 3, the NSE index is weighted towards the effect of large values (Krause *et al.*, 2005). Acknowledging this

behaviour of the NSE index, it is still used in the performance evaluation of the lake level change model. However, the performance of the model is also evaluated through qualitative visual examination of timeseries and scatterplots.

5.2 Calibration

Calibration of the model was carried out during the model development, with the final parameter values presented in Table 4-1. In this section a visual inspection and interpretation of plots with the actual ΔL_{48} and the $\widehat{\Delta L}_{48}$ from the model calibration are presented as the basis for the validation evaluation.

The timeseries plot, Figure 5-1, for the years 2008 and 2009, displaying the ΔL_{48} and $\widehat{\Delta L}_{48}$ for Lake Wanaka, shows that the model calibration does reasonably well in fitting both positive and negative lake level changes. The model under-fits many of the large lake level rises, ΔL_{48} > 0.5m and fits the small lake level rises well, ΔL_{48} < 0.5m, with minor under-prediction and over-prediction occurring. The calibrated lake level recession appears to fit to the observed lake level recession well, just underestimating the more rapid lake level recession rates around May 2009.

The model failed to fit some lake rises altogether, as can be seen in Figure 5-1 for a large rise in March 2008 and another smaller rise occurring November 2009. These failed predictions were common throughout the whole calibration dataset and largely reflect the model assumption of rain gauge data being spatially representative of catchment rainfall. Another factor might be the inability of the model to predict snowmelt river water entering the lake, which at times is so great it causes the lake level to rise without significant rainfall.

The calibration results for Lake Wakatipu followed a similar pattern to Lake Wanaka throughout, also fitting the observed data reasonably well, under-fitting large lake level rises, ΔL_{48} > 0.25m, fitting better to the small rises, ΔL_{48} < 0.25m, and unable to estimate certain lake level rises throughout the year (Fig. 5-2).

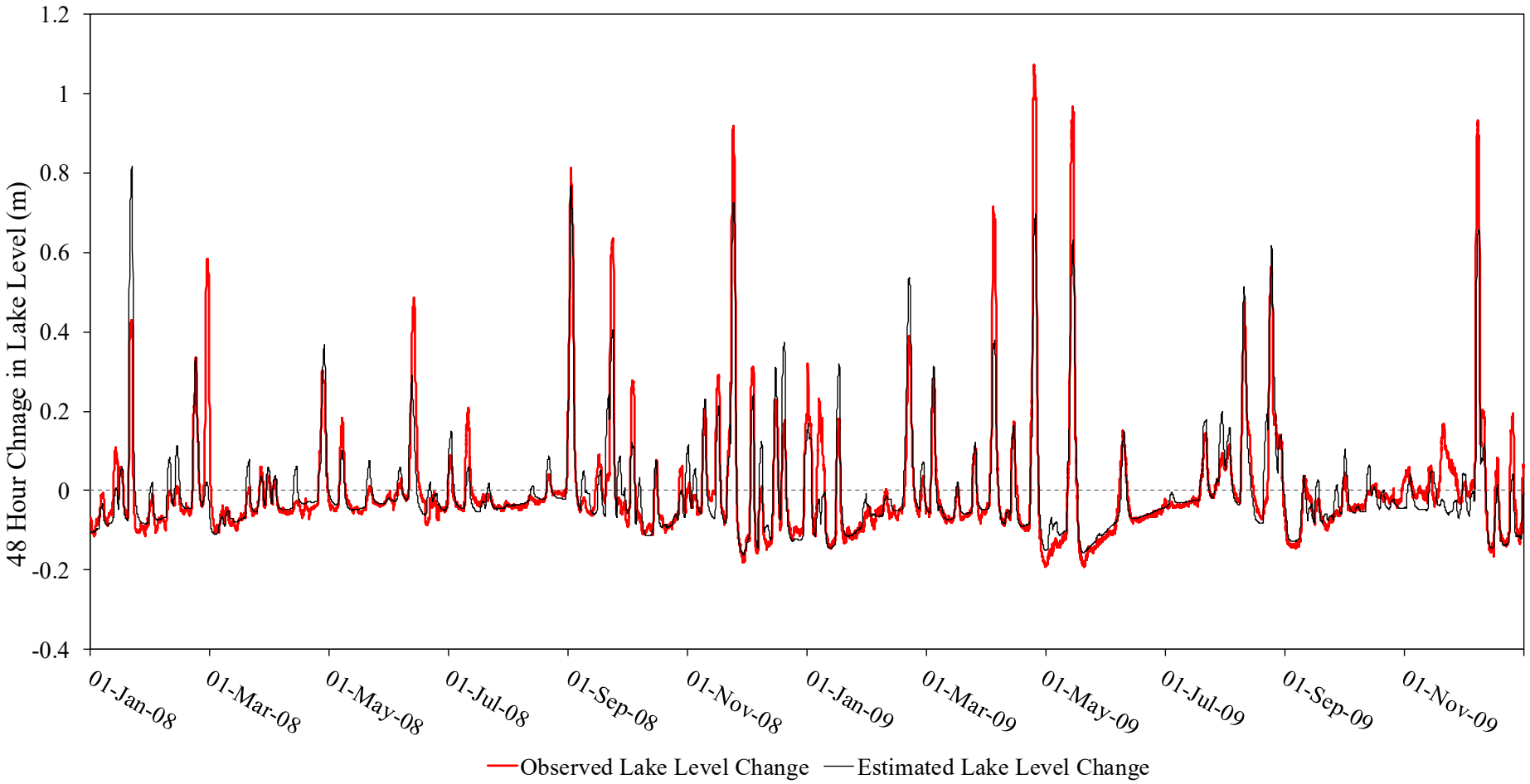

Figure 5-1: Time series plot of observed lake level change and the calibration-fitted lake level change, for 48-hours ahead forecasts for Lake Wanaka. The forecasts are for every hour of the years 2008 and 2009.

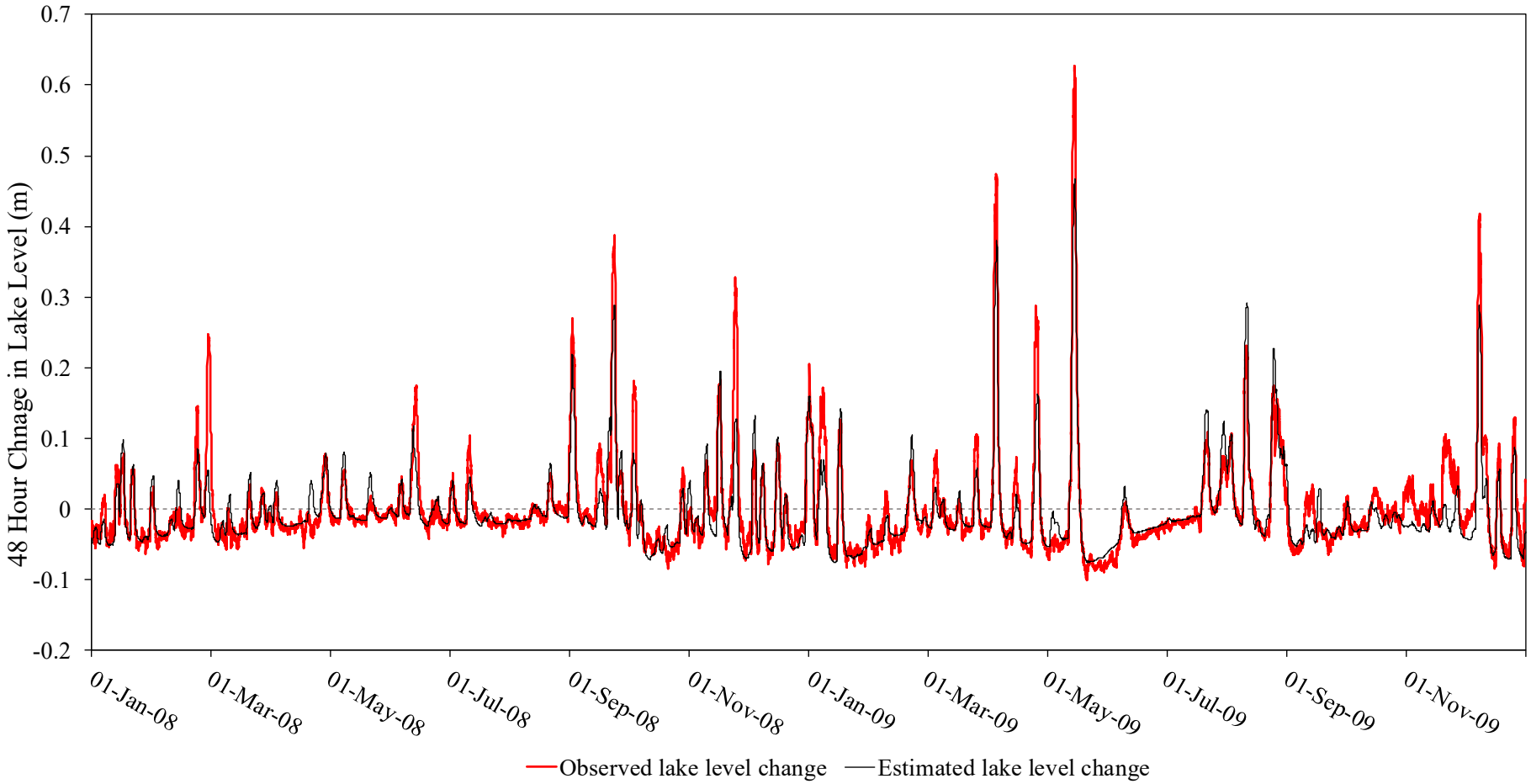

Figure 5-2: Time series plot of observed lake level change and the calibration-fitted lake level change, for 48-hours ahead forecasts for Lake Wakatipu. The forecasts are for every hour of the years 2008 and 2009.

The seasonal scatterplots for ΔL_{48} against $\widehat{\Delta L}_{48}$ for the calibration of the model applied to Lake Wanaka (Fig. 5-3), for the whole calibration period, present similar findings to the timeseries plot (Fig. 5-1). The loops of the data points reflect individual lake level rises, as seen in the timeseries, with the adjacent datapoints in the loops representing model predictions made at adjacent hourly timesteps. Several of the NSE index values are therefore based on a few lake level rise events, despite numerous data points.

The better the model calibration to the lake level rise, the closer the loop data points will be to the 1:1 line. The lake level rises which are not fitted by the model appear as the loops moving horizontally away from the 1:1 line. The seasonal scatterplots also show the model under-predicts many of the lake level rise peaks, occurring more often in Autumn and Winter (Fig. 5-3).

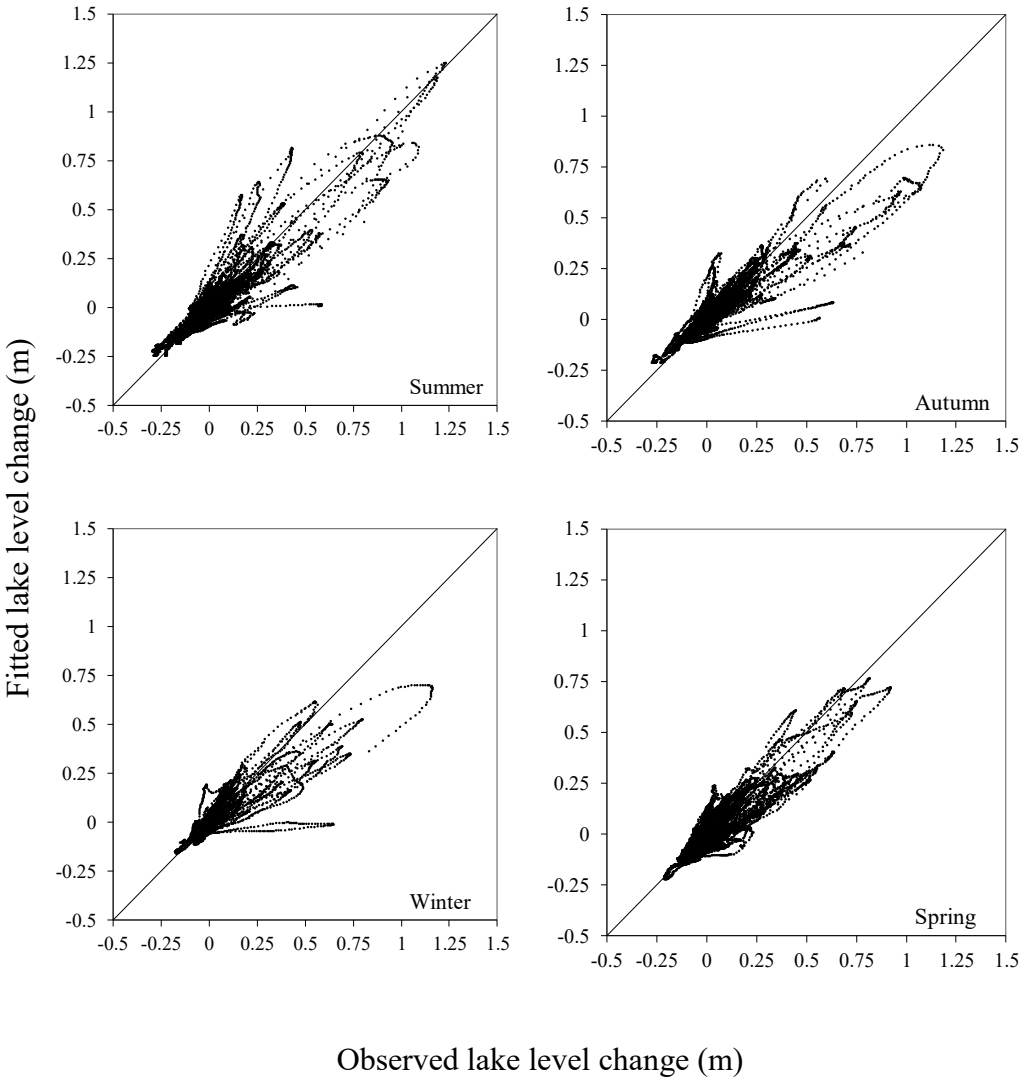

Figure 5-3: Seasonal scatterplots of the observed lake level changes against the calibration-fitted lake level changes at a lead-time of 48 hours for Lake Wanaka for the years 2006 to 2013. Diagonal straight line is the 1:1 line.

5.3 Hindcast Validation

The hindcast validations for both lakes have similar, with nil-minimal change, validation NSE values as their respective NSE calibration value, for 48 hour lead-times (Table 5-1). These results indicate a degree of predictive ability subject to forecast rainfall being close to the rain gauge rainfall.

Table 5-1: Nash-Sutcliffe efficiency values for calibration and the hindcast validation for Lakes Wanaka and Wakatipu, at a lead-time of 48 hours.

	Calibration	Validation
Lake Wanaka	0.81	0.80
Lake Wakatipu	0.82	0.82

Breaking the validation NSE values into seasons gives more of an insight into how the model is performing at different times of year (Table 5-2). For Lake Wanaka the summer NSE value dropped down to 0.75 for the hindcast validation from a value of 0.84 in the calibration. For autumn the Wanaka validation NSE value was higher at 0.90, actually up from the calibration value of 0.82. For winter the hindcast calibration and validation NSE values had minimal change and for spring the NSE values dropped down to 0.62 from a value of 0.79 in the calibration. It is to be expected that the NSE value for spring may be low given the volatile influences of snowmelt during spring which were not modelled, the high NSE value for the calibration may have been because the few large well fitted lake level rises were not significantly influenced by snowmelt.

For Lake Wakatipu, the NSE validation values for summer, autumn and winter are all slightly up from the NSE values in the calibration and spring dropped down to a hindcast validation value of 0.60 from 0.75 in the calibration.

For all seasons the NSE values indicate that the high lake level changes are well estimated in comparison to the benchmark model of no lake level change. Spring was not estimated as well as the other seasons, although the model still performed much better than the benchmark model.

Table 5-2: Nash-Sutcliffe seasonal values for calibration and hindcast validation for Lakes Wanaka and Wakatipu, at a lead-time of 48 hours.

	Lake Wanaka		Lake Wakatipu	
	Calibration	Validation	Calibration	Validation
Summer	0.84	0.75	0.85	0.87
Autumn	0.82	0.90	0.83	0.87
Winter	0.78	0.77	0.85	0.88
Spring	0.79	0.62	0.76	0.60

NSE values were calculated for periods when the model was estimating a lake level recession ($\widehat{\Delta L}_{48} < 0$). Table 5-3 shows the validation NSE values both improved and worsened in comparison to the calibration NSE values. For both lakes the estimated lake level recession had the lowest NSE validation values in spring, which also had the lowest NSE values during the calibration period. During spring snowmelt may raise the inflows into the lakes independently of recent rainfall, the model did not account for this causing the NSE values to be low. Although the model does not account for snowmelt, the model estimated the lake level recessions better than the benchmark model of no lake level change.

Table 5-3: Nash-Sutcliffe seasonal values for calibration and hindcast validation for Lakes Wanaka and Wakatipu, at a lead-time of 48 hours. Only for times when $\boldsymbol{\widehat{\Delta L}_{48} < 0}$.

	Lake Wanaka		Lake Wakatipu	
	Calibration	Validation	Calibration	Validation
Summer	0.87	0.83	0.83	0.86
Autumn	0.87	0.93	0.87	0.85
Winter	0.67	0.83	0.87	0.88
Spring	0.53	0.37	0.42	0.61

The seasonal scatterplots of ΔL_{48} against $\widehat{\Delta L}_{48}$ for the hindcast validation help with qualitative assessment of the model performance for lake level rises. In summer and winter for Lake Wanaka the hindcast validation NSE values were similar (Table 5-2). However, the scatterplots show the season-defined observed lake level changes were not estimated in the same manner, with the model underestimating two large lake level rises in winter and for summer the model over- and underestimating large lake level rises (Fig. 5-4). While no definite conclusion can be reached through the over- and underestimation of just two large lake level rises, this highlights the importance of evaluating the models further than the quantitative simple index values, for an informative understanding of model performance.

The scatterplots shown in Figure 5-4 show the model predominantly underestimates large lake level rises in Lake Wanaka, with most of the data points sitting below the 1:1 line. The smaller lake level rises in summer, winter and autumn are better estimated with the data points all closer to 1:1 line, although for spring the smaller lake level rises are mostly underestimated.

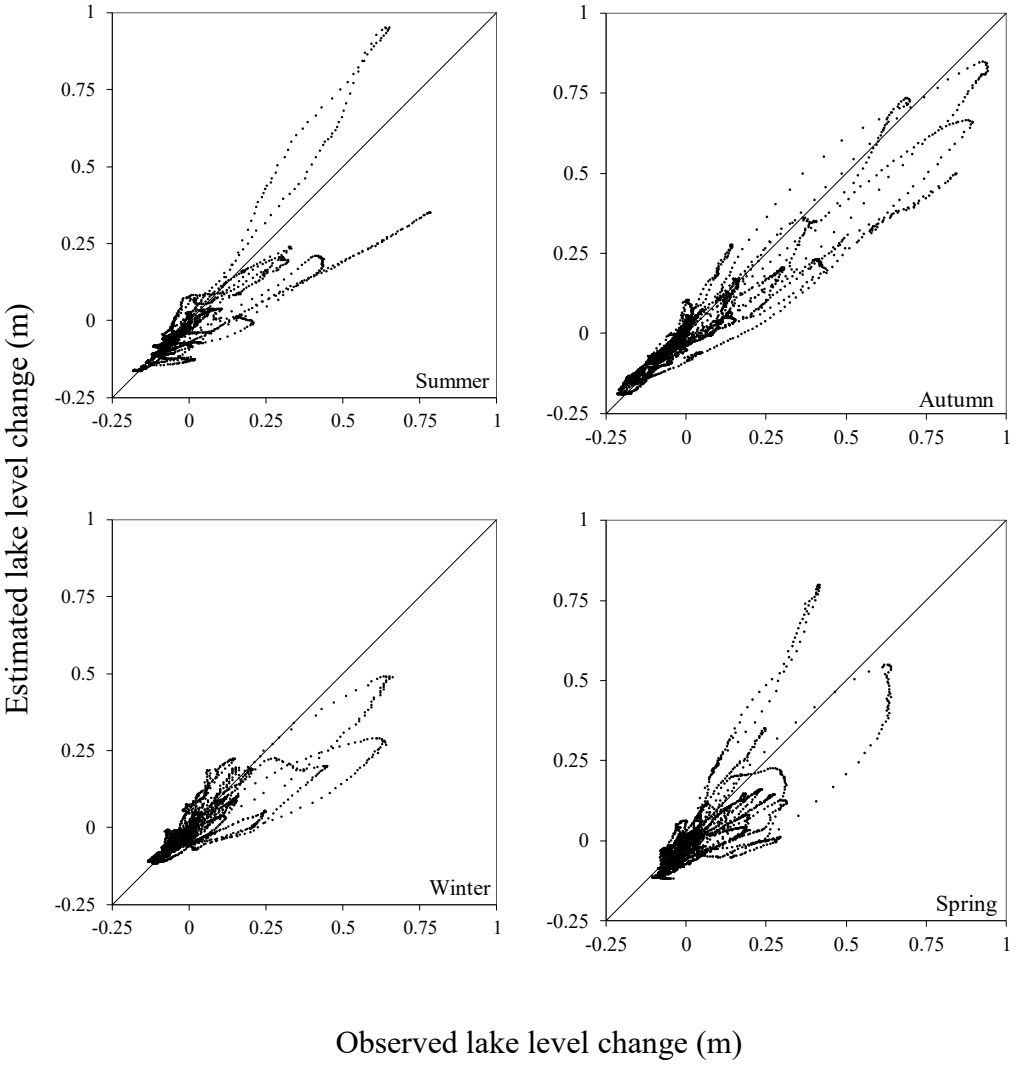

Figure 5-4: Seasonal scatterplots of the observed lake level changes against the estimated lake level changes at a lead-time of 48 hours for Lake Wanaka for the hindcast validation period of the years 2015 to 2016. Diagonal line is the 1:1 line.

The seasonal scatterplots of ΔL_{48} against $\widehat{\Delta L}_{48}$ for the hindcast validation for Lake Wakatipu, show the model appears to behave differently than Lake Wanaka. For summer and winter the large lake level changes occurring in Lake Wakatipu are well estimated with the data points following closely to the 1:1 line (Fig. 5-5), in contrast to the over- and underestimation of large lake levels changes present during summer and winter in Lake Wanaka (Fig. 5-4). For autumn the lake level changes in Lake Wakatipu are well estimated with the datapoints all following closely to the 1:1 line, apart from one obvious major underestimation where the model does not appear capture a lake level rise, shown by the data points moving horizontally away from the 1:1 line, which did not occur during autumn in Lake Wanaka (Fig 5-4). The estimated lake level changes for spring in Lake Wakatipu are underestimated.

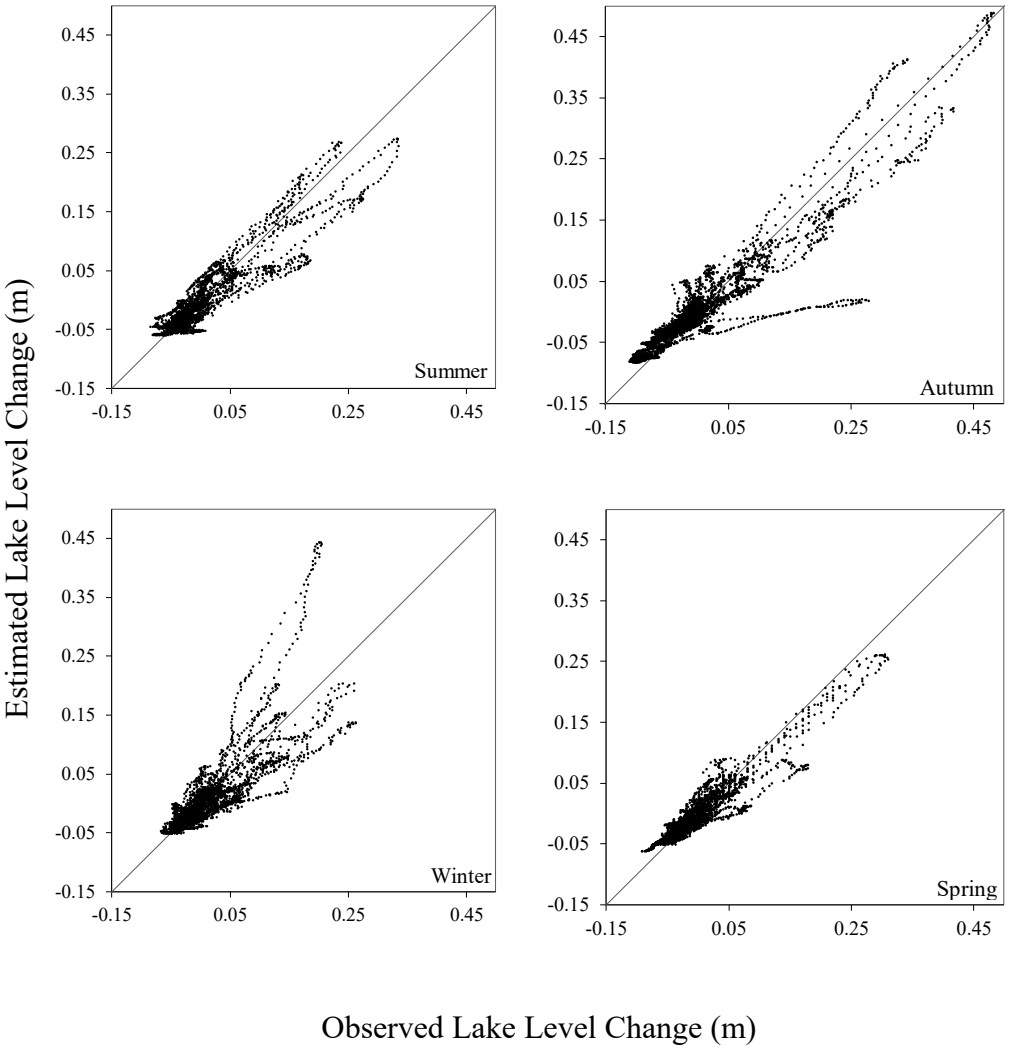

Figure 5-5: Seasonal scatterplots of the observed lake level changes against the estimated lake level changes at a lead-time of 48 hours for Lake Wakatipu for the hindcast validation period of the years 2015 to 2016. Diagonal line is the 1:1 line.

Inspecting the timeseries plots of ΔL_{48} and $\widehat{\Delta L}_{48}$, for Lake Wanaka and Wakatipu helps to further understand the model performance. For Lake Wanaka it is clear from Figure 5-6 that the model underestimates many of the lake level rise peaks, as was seen in the scatterplots (Fig. 5-4). Although the model does not perfectly predict the magnitude of the $\widehat{\Delta L}_{48}$, the timeseries shows the general overall pattern of the $\widehat{\Delta L}_{48}$ for Lake Wanaka was approximately consistent with the timing and behaviour of the observed lake level changes, during the hindcast validation period.

For spring, the hindcast validation scatterplots for Lake Wanaka revealed many of the small lake level changes were underestimated. There was also a large overestimation occurring. The time-series plot shows most of the underestimations of small lake level rises occur around the same time in October 2015, while the large overestimation occurred in October 2016.

When Lake Wanaka's level recedes $(\Delta L_{48} < 0)$, the model estimates the lake level recession well. The period between December 2015 and January 2016 illustrates the model is capable of estimating lake level recession over a range of values. However, the model does fail to estimate the minor lake level rises which occurred during this time.

The rapid lake level recession (high negative lake level change values) which occurred at the end of May 2016 is slightly underestimated, though the rapid lake level recession which occurred in May 2015 of the same magnitude was well estimated (Fig. 5-6).

For Lake Wakatipu the model also estimated most lake level recession periods well, apart from slightly underestimating the rapid lake level recessions in both years (Fig. 5-7). The timeseries for Lake Wakatipu shows the model underpredicts many lake level rise peaks but not to the same extent as seen for Lake Wanaka. Near the beginning of May, in both 2015 and 2016, Lake Wakatipu experienced large lake level increases and in both years the model estimated these well. This contributes to the high NSE value of 0.90 for autumn in the hindcast validation (Table 5-2). The observed autumn lake level rise which the model failed to estimate is seen in the time-series plot occurring in March 2016, the corresponding rise in Lake Wanaka was well estimated (Fig. 5-6).

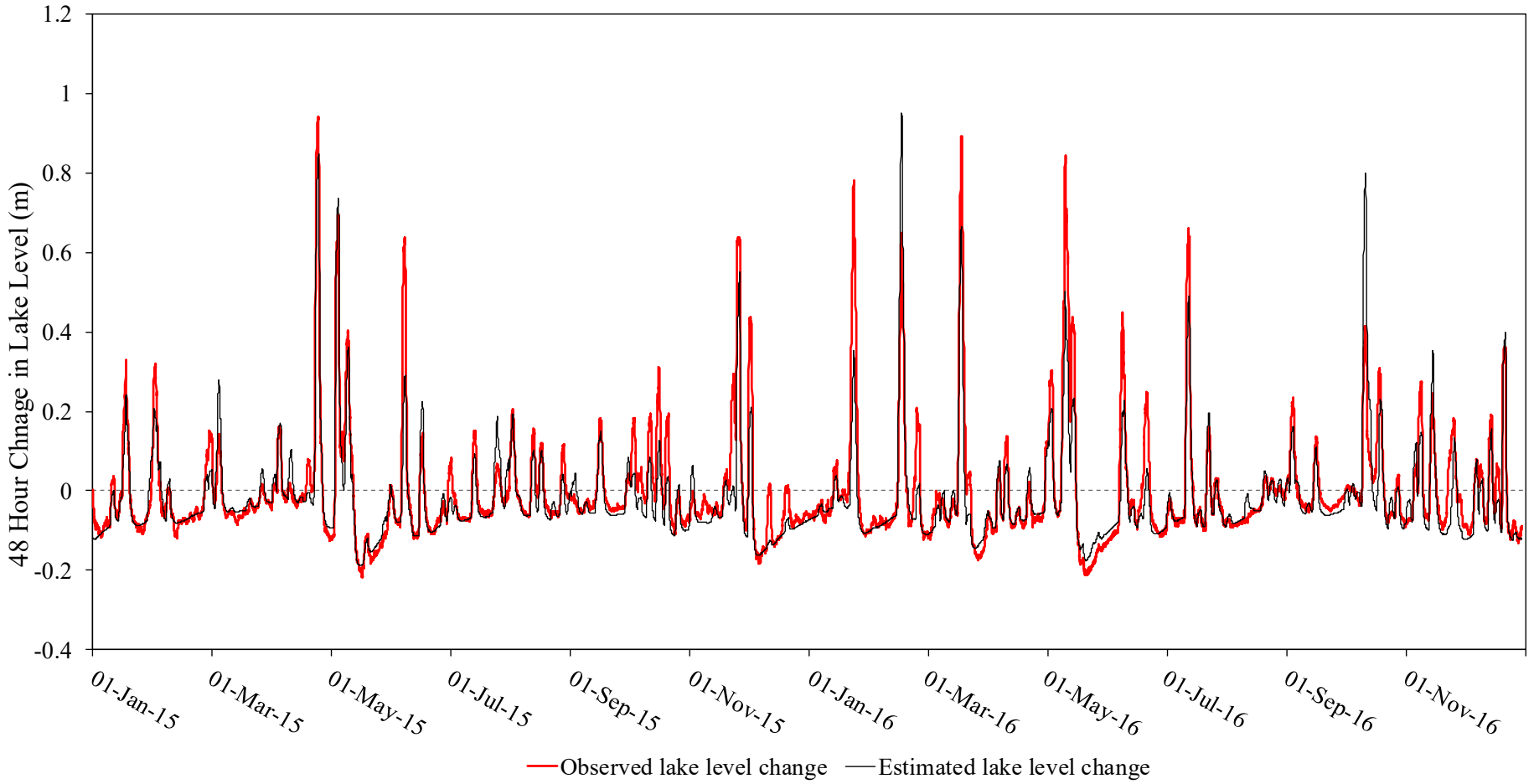

Figure 5-6: Hindcast validation time series plot of observed Wanaka lake level change and model-predicted lake level change, 48 hours ahead. Model predictions were made every hour of the years 2015-2016.

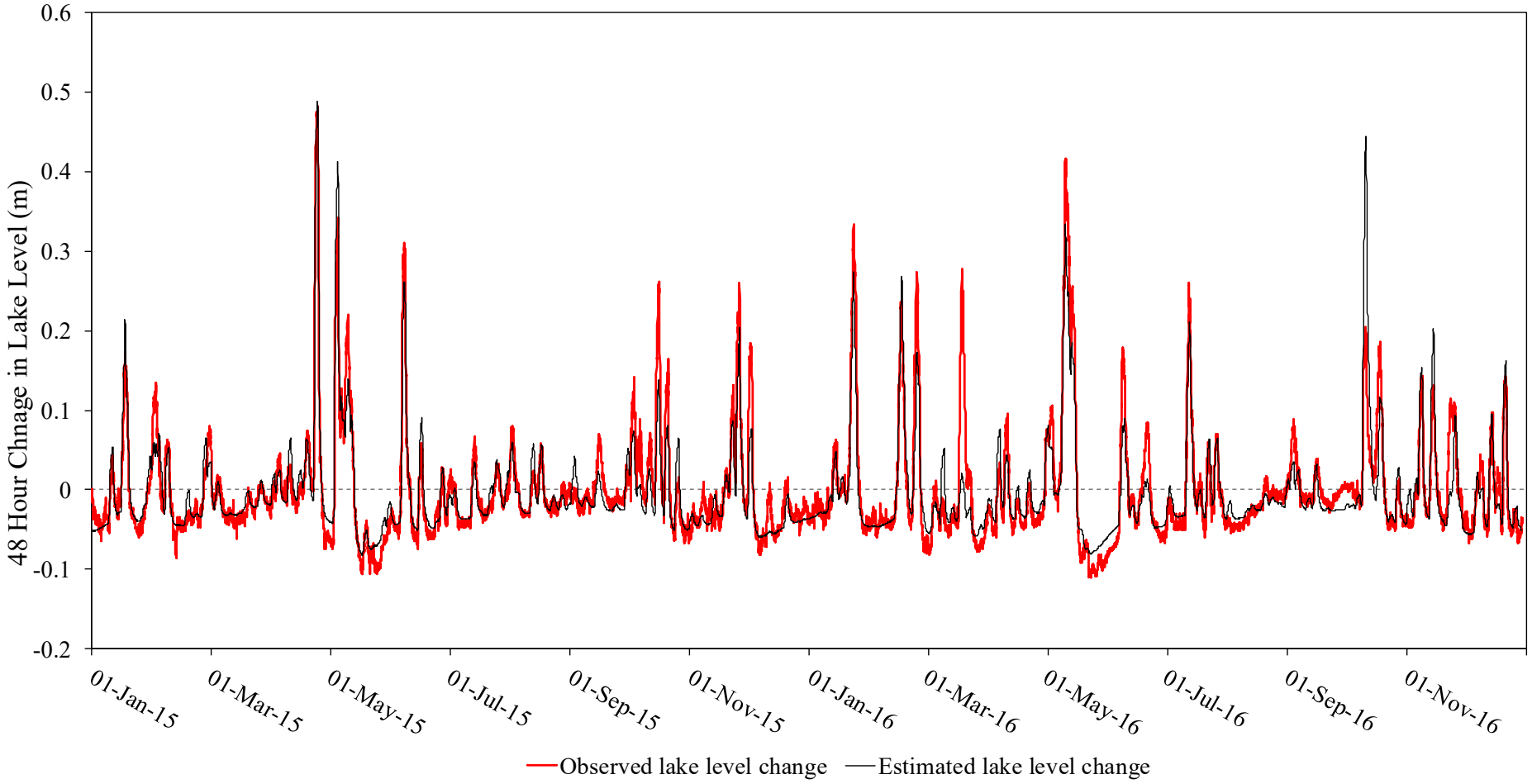

Figure 5-7: Hindcast validation time series plot of observed Wakatipu lake level change and model-predicted lake level change, 48 hours ahead. Model predictions were made every hour of the years 2015-2016

5.3.1 Rain Gauge Representativeness

During the development of the model it was common to see observed lake level rises for both lakes, but with no corresponding recorded rainfall and therefore no predicted lake level rise. Yet it usually occurred in both lakes and was interpreted as the possibility of rainfall having had occurred at high elevations above rain gauges or due to snowmelt. However, when the model was applied to Lake Wanaka it captured a large lake level rise in March 2016 but when applied to Lake Wakatipu the model did not capture the corresponding rise. To investigate further, time series plots from 1 to 48 hours for Lake Wanaka and Lake Wakatipu were plotted, where t_0 begins at 2am 17th March 2017 (Fig. 5-8 and 5-9).

The rain gauges selected for Lake Wanaka captured a storm occurring and therefore the model estimated the lake level to rise steadily over the next 48 hours (Fig. 5-8). The rain gauges selected for Lake Wakatipu, however, only recorded a small amount of rainfall, just enough for the model to estimate that the lake level would not recede over the next 48 hours but not enough for the model to estimate the significant rise which was observed in the lake (Fig. 5-9). The value for the rainfall proportion, α, for both lakes during this time period was equal to 1, and therefore the large difference between the effective rainfall for the two lakes during this event is not a result of low temperatures reducing α (Eq. 12).

This example demonstrates the reliance the model has on the accuracy of the rain gauge data being representative of the whole catchment. It is likely the storm recorded in March 2016 in the Lake Wanaka catchment by the rain gauges Makarora and Matukituiki, also occurred over in the Lake Wakatipu catchment but not in the area of the rain gauges, Dart and Paradise (Fig. 2-2). Therefore, in this case the rain gauges, Makarora and Matukituiki, would have likely produced better estimations of the lake level rise in Lake Wakatipu than the rain gauges, Dart and Paradise.

This is not to say that Makarora and Matukituiki should be used for Lake Wakatipu instead of Dart and Paradise but simply highlights the poor spatial representation of the rain gauges used in the model which diminishes predictive power of the model. A mixed weighting of Dart and Paradise works most of the time for forecasting the lake level rises in Lake Wakatipu, however, as seen here not all the time.

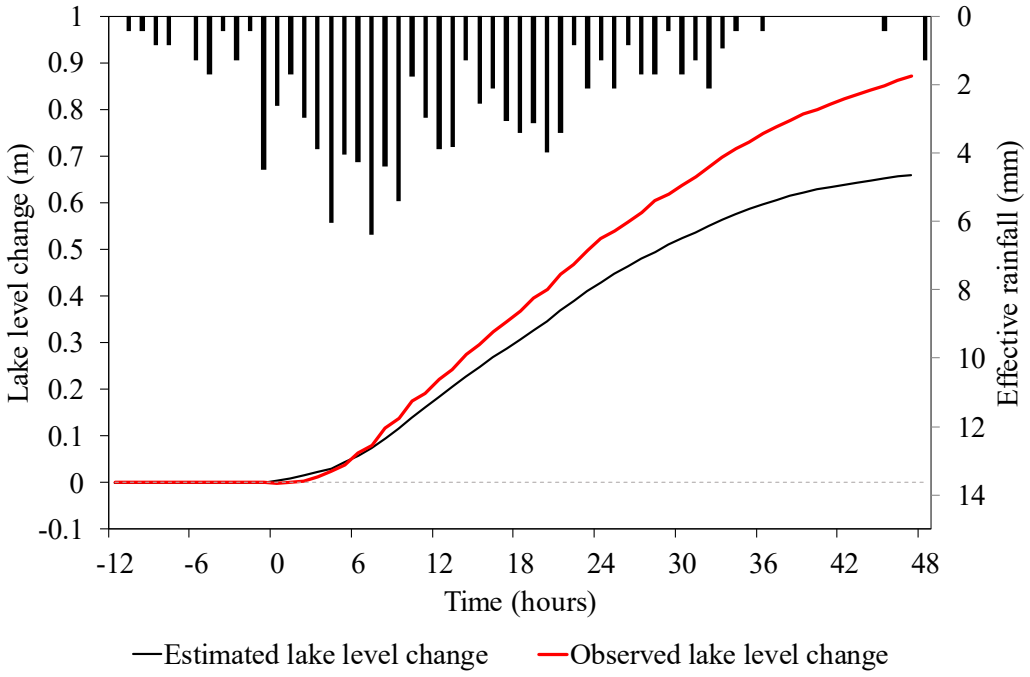

Figure 5-8: A timeseries showing the estimated and observed lake level changes in Lake Wanaka for each lead-time, t > 0, for a lake level change estimation made at 2am on the 17th March 2016. The contributing rainfall is also plotted at each time-step relevent to t_0.

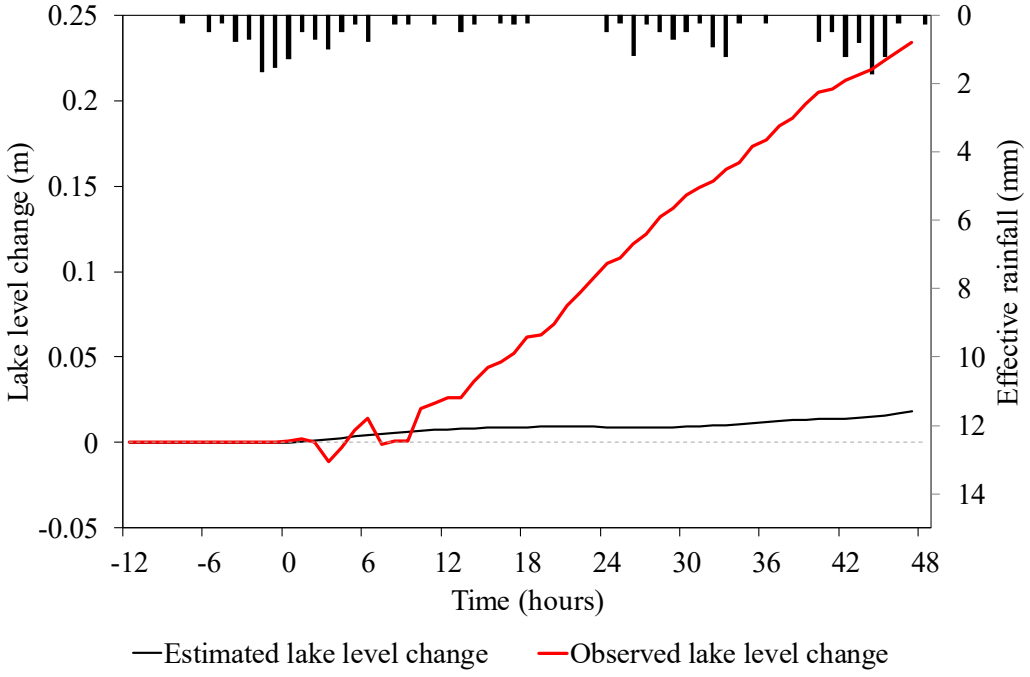

Figure 5-9: A timeseries showing the estimated and observed lake level changes in Lake Wakatipu for each lead-time, t > 0, for a lake level change estimation made at 2am on the 17th March 2016. The contributing rainfall is also plotted at each time-step relevent to t_0.

5.4 Conclusion

Overall the hindcast validation for the model applied to the two lakes shows the model can simulate the observed lake level changes reasonably well for both lakes, given the hindcast gauge rainfalls. Large lake level rises were found to be mostly underestimated for both lakes but more common in Lake Wanaka. The smaller lake level changes tended to be well estimated with a balance of both over and under-estimation apart from in spring where under-estimation was dominant. The underestimation in spring highlights the fact the model does not have a snow melt component and for some years the model will predominantly underestimate the lake level rise. Over-prediction is still possible during spring, however, as seen in the year 2016.

The lake level recessions were well estimated in both lakes but lacked accuracy for the rapid lake level recessions, mainly underestimating the recession rates. This suggests that the rapid lake level recession periods used in the calibration of D_f, to estimate parameters a, b and c were influenced by recent rainfall in the catchment and therefore $I_f \neq 0$, causing underestimation of D_f for high lake levels (Eq. 4).

This is a complex problem to solve because periods of rapid lake level recession tend to occur straight after periods of high lake level rise, which caused the lake level to be so high in the first place. Therefore, differentiating between D_f and I_f is difficult at high lake levels because the inflow is still very high from the recent rainfall. The problem cannot be solved backwards because as seen in the hindcast validation and calibration, I_f is subject to large errors during high lake level rises. Attempts to correct this during calibration failed, probably because the underestimation D_f balanced out the underestimation I_f. This is perhaps acceptable, given that the goal of the model is high predictive power and not physical simulation.

On a time scale of a few days, the rain gauge rainfalls are not representative of the whole catchment's rainfall. This is inevitably a model weakness in that the model was developed on the assumption the rain gauge rainfall is representative of the whole catchment rainfall. The hindcast validation of the model highlighted large output errors resulting from this assumption, presenting an example of a lake level rise occurring in Lake Wakatipu which was not estimated by the model due to poor catchment rainfall representation by the rain gauges.

Chapter 6 - Forecast Validation

6.1 Introduction

Chapters 4 and 5 used recorded rain gauge and temperature data for the development, calibration and hindcast validation of the model. However, once in operation the model will not have access to recorded rain gauge and temperature data beyond the current time. Forecast rainfall and temperature data will therefore need to be used as an input into the model instead of recorded rainfall and temperature.

It is well known rainfall forecasts are subject to large errors. As a consequence, there can be much greater model forecast errors (Kobold, 2005). This chapter presents the forecast validation results for lake level change predictions when forecast rainfall and temperature are used in model input. The results from these validations will give a more realistic test of how the model will perform in later operational use.

6.2 Forecast Data

Forecast rainfall and temperature data were obtained for January 2017 to November 2018, through Contact Energy produced by Blueskies. The forecasts are updated every 12 hours beginning at 7am and 7pm every day and extend out for the next 66 hours. The forecast rainfall gives a single value of rainfall depth as the spatial average depth across the whole of the Upper Clutha catchment area. The forecast temperature gives two temperatures at 1500 m and 750 m elevation with a lapse rate value.

The forecast data are at a three hourly temporal resolution. As the model was designed to work in hourly timesteps the forecasts were altered to match. For example, if the forecast predicts 3mm of rain from 12pm to 3pm, 1mm of rain was placed into the timesteps 12pm to 1pm, 1pm to 2pm, and 2pm to 3pm. Temperature was kept the same across all three hours. It should be noted there were several missing forecasts in the dataset, these periods were removed from the analysis.

6.2.1 Forecast rainfall

The rain gauges used for rainfall inputs into the model during development are situated at low elevations in their respective catchments (Fig. 2-2) and therefore

typically record rainfall depth values much lower than what the spatial average rainfall depth of the whole catchment would be or in this case what the forecast spatial average rainfall depth is. As the model was developed and calibrated using recorded data and not forecast data, the association between forecast rainfall and gauge rainfall first needs to be estimated. The forecast rainfall is then transformed to estimated respective gauge rainfall for model input.

To achieve this, the total forecast rainfall over the available period was compared with the corresponding recorded gauge totals. This comparison produced gauge-specific weight values (ω_f) to adjust the forecast rainfalls for input into the model (Eq. 8). It was found the forecast rainfall needed to be multiplied by the weight value of 0.64 for Lake Wanaka and by 0.57 for Lake Wakatipu.

Li *et al.* (2017) applied forecast rainfall in this way to a hydrological model calibrated on rain gauge data, with a correction required for forecast bias which increased with lead time. To check against possible similar bias in the present study, ω_f values were calculated across five lead-times of 12 hour periods. Although there appears to be a slight decrease over the lead-times in ω_f, it is not great enough to suggest the forecast rainfall has a bias for overpredicting with increasing lead-time, this could simply be the result of one forecast with a large error (Fig. 6-1).

The lead-time period for forecast rainfall from 49 to 60 hours needed to be included in the forecast and recorded rainfall comparison (Fig. 6-1) because it is used within the model, as the forecasts are only updated every 12 hours. For example, the forecast rainfall value used in the model to calculate P, 48 hours ahead (P_{48}) for a lake level change forecast made at 7am, will be the forecast rainfall value at the lead-time of 48 hours, from the rainfall forecast which has just been updated. However, when the model runs again at 6pm later that day the rainfall value used to calculate P_{48} will be the forecast rainfall at the lead-time of 59 hours, from the same rainfall forecast made earlier that day.

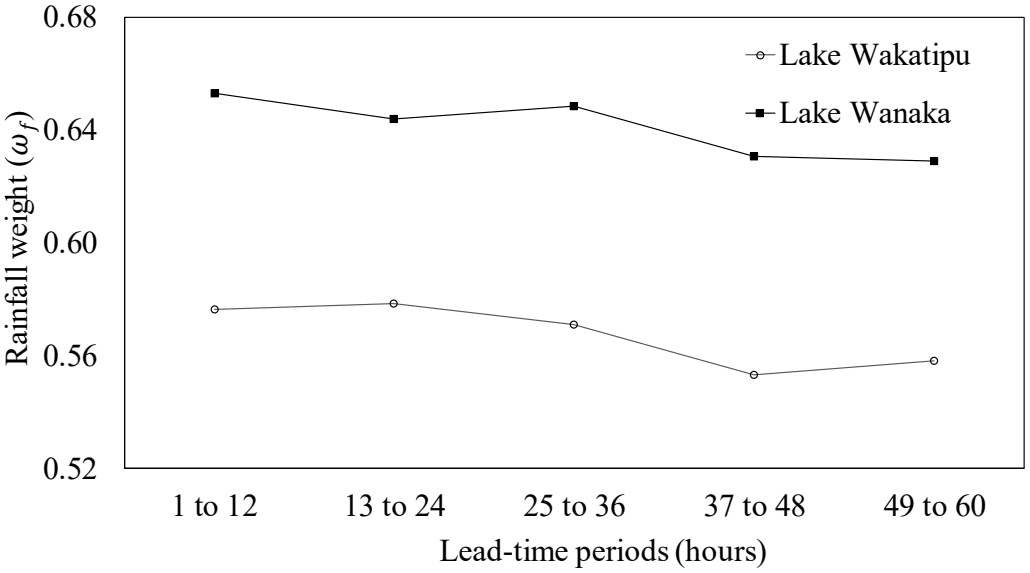

Figure 6-1: The rainfall weight required to be applied to the forecast rainfall to match the recorded rainfall values, across five lead-times periods.

The *P* calculated from recorded rainfall for Lake Wakatipu accumulated over 24-hour periods is plotted against the *P* calculated from forecast rainfall for the same period to visually inspect the error of the forecast rainfall (Fig. 6-2). The left scatterplot in Figure 6-2 is the forecast *P* accumulated over the lead-times 1 to 24 hours and the right scatterplot is forecast *P* for the same 24 hour period, this time accumulated at the forecast lead-times 25 to 48 hours. The scatterplots reveal the error associated with the forecast rainfall through the scatter of the datapoints, which increases with the increased lead-time.

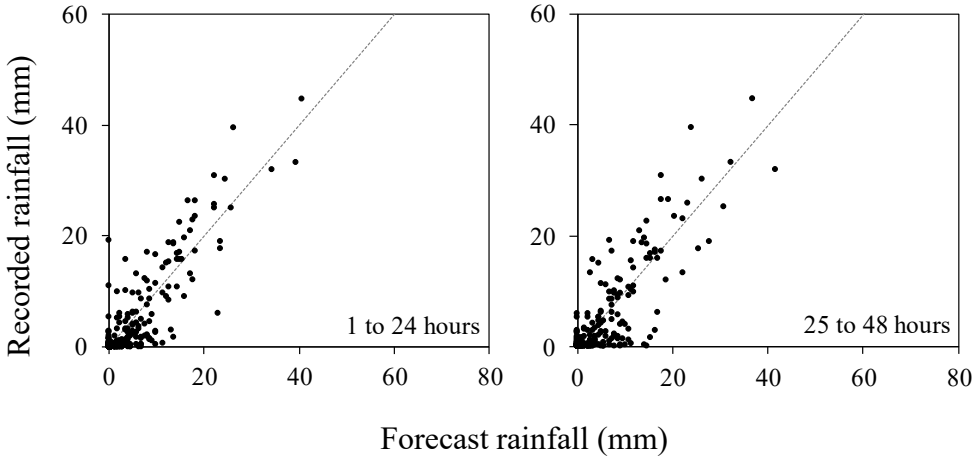

Figure 6-2: Scatterplots with recorded rainfall total, for a period of 24 hours, plotted against the adjusted rainfall forecast for the same period. The left scatterplot has the forecast rainfall at lead-times 1 to 24 hours and the right scatterplot has the forecast rainfall at lead-times 25 to 48 hours.

6.2.2 Forecast temperature

The forecast data provides two temperatures at different elevations, 750 m and 1500 m, and the calculated lapse rate. As the recorded temperature used for development and calibration of the model was recorded at Matukituki at an elevation of 300 m, the forecast temperature at the elevation of 750 m, T_{750}, is adjusted using the following equation:

$$T_{300} = T_{750} + 4.5 \times \frac{\Delta C°}{100m} \quad (15)$$

where $\frac{\Delta C°}{100m}$ is the lapse rate provided in C° per 100m, and 4.5 is the difference in elevation (×100 m) between the T_{750}, and the model input temperature at 300 m elevation, T_{300}.

6.3 Forecast Validation

The overall forecast validation NSE values for the two lakes dropped considerably from the hindcast calibration NSE values as seen in Table 6-1, reflecting the effect of rainfall and temperature forecasts. However, the values indicate the model still manages to do better than the benchmark model of current water level.

Table 6-1: Nash-Sutcliffe efficiencies for the hindcast calibration and forecast validation of the lake level change model applied to Lakes Wanaka and Wakatipu, at a lead-time of 48 hours.

	Calibration	Validation
Lake Wanaka	0.81	0.58
Lake Wakatipu	0.82	0.64

Table 6-2 indicates forecast validation NSE values drop from the calibration NSE over all seasons. Winter had the highest NSE values, followed by summer, autumn, and spring with the lowest values. Spring was not expected to do well for either lake with the influences of snow melt and the poor hindcast validation NSE values for the season. For Lake Wanaka, autumn had a low NSE value of only 0.50, after having highest NSE value in the hindcast validation of 0.90 (Table 5-2).

Table 6-2: Nash-Sutcliffe efficiency seasonal values for the hindcast calibration and forecast validation of the model applied to Lakes Wanaka and Wakatipu, at a lead-time of 48 hours.

	Lake Wanaka		Lake Wakatipu	
	Calibration	Validation	Calibration	Validation
Summer	0.84	0.70	0.85	0.70
Autumn	0.82	0.50	0.83	0.64
Winter	0.78	0.77	0.85	0.83
Spring	0.79	0.48	0.76	0.50

Figures 6-3 and 6-4 show the seasonal scatterplots of ΔL_{48} against $\widehat{\Delta L}_{48}$ for the forecast validation of the model applied to Lakes Wanaka and Wakatipu. The model appears to give a similar pattern of results for both lakes. Across all four seasons the model underpredicts the lake level changes with the majority of the data points in the scatterplots situated below the 1:1 line. There is, however, one large over-estimation of lake level which occurred in summer. The scatterplots reveal the lack of lake level rises occurring in the forecast validation period, especially when compared to the hindcast validation scatterplots (Fig. 5-4 and 5-5). This shows the NSE values are driven by only a few high data points and are likely not appropriate for evaluating the forecast model, due to the lack of lake level rises. The scatter of the data points in the forecast validation scatterplots is also significantly increased compared to the hindcast validation results.

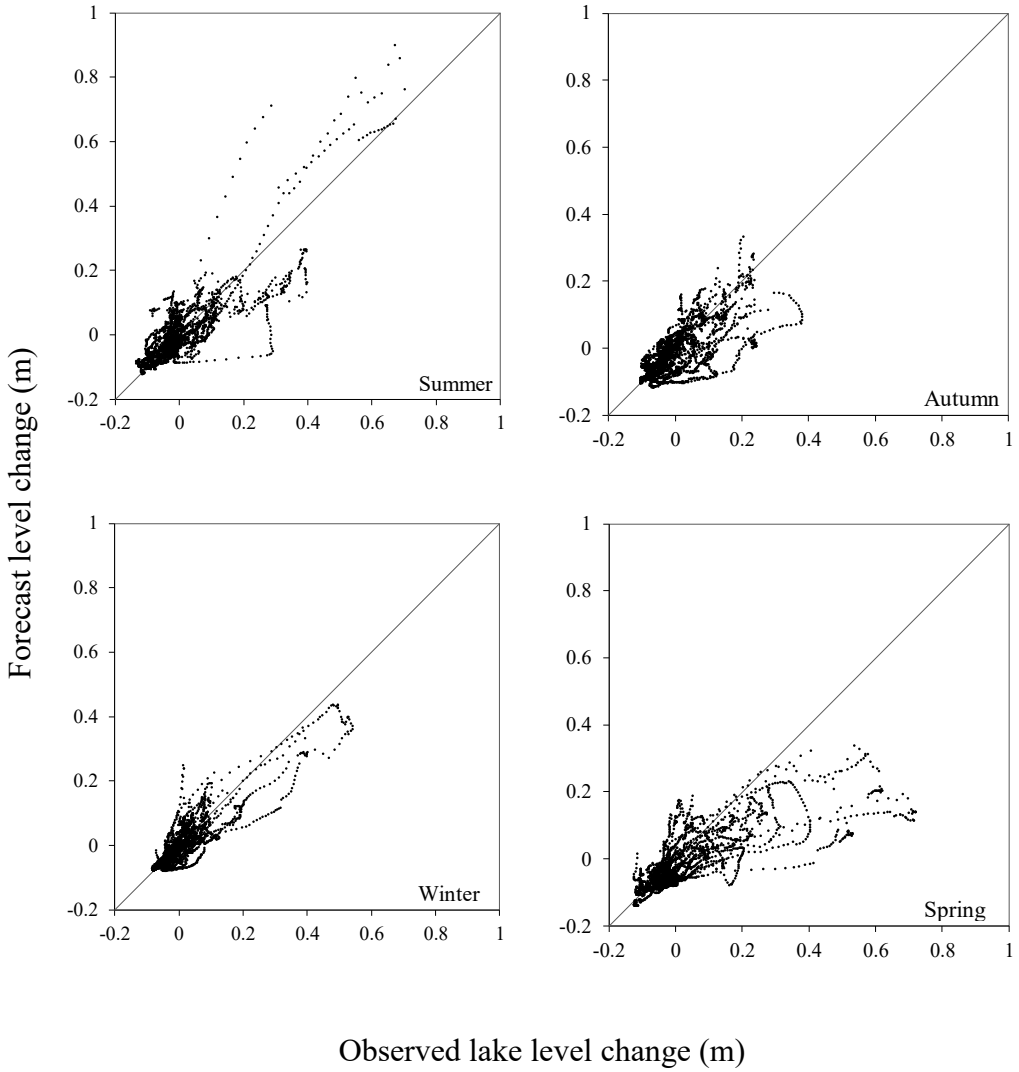

Figure 6-3: Seasonal scatterplots of the observed lake level changes against the forecast lake level changes at a lead-time of 48 hours for Lake Wanaka for the forecast validation. The diagonal straight line is the 1:1 line.

The scatterplots for winter suggest a subtle difference between the lake behaviours, with Lake Wakatipu only having one large distinguishable lake level rise of around 0.45m which was slightly under-predicted (Fig. 6-4). In contrast, Lake Wanaka recorded two clearly distinct rises during winter, both of which were under-predicted (Fig. 6-3).

For autumn, no distinct large lake level rises occurred in either lake, hindering the model performance evaluation for the season. A few lake level rises occurred in spring, with most the data points situated below the 1:1 line, allowing for a more confident evaluation of seasonal effects, suggesting that season-based forecasts are prone to underestimation. However, how much of the underestimation is due to the model not modelling snowmelt, or a bias in the model is unable to be distinguished. The overall underestimation across all seasons suggests the model is biased towards underestimation.

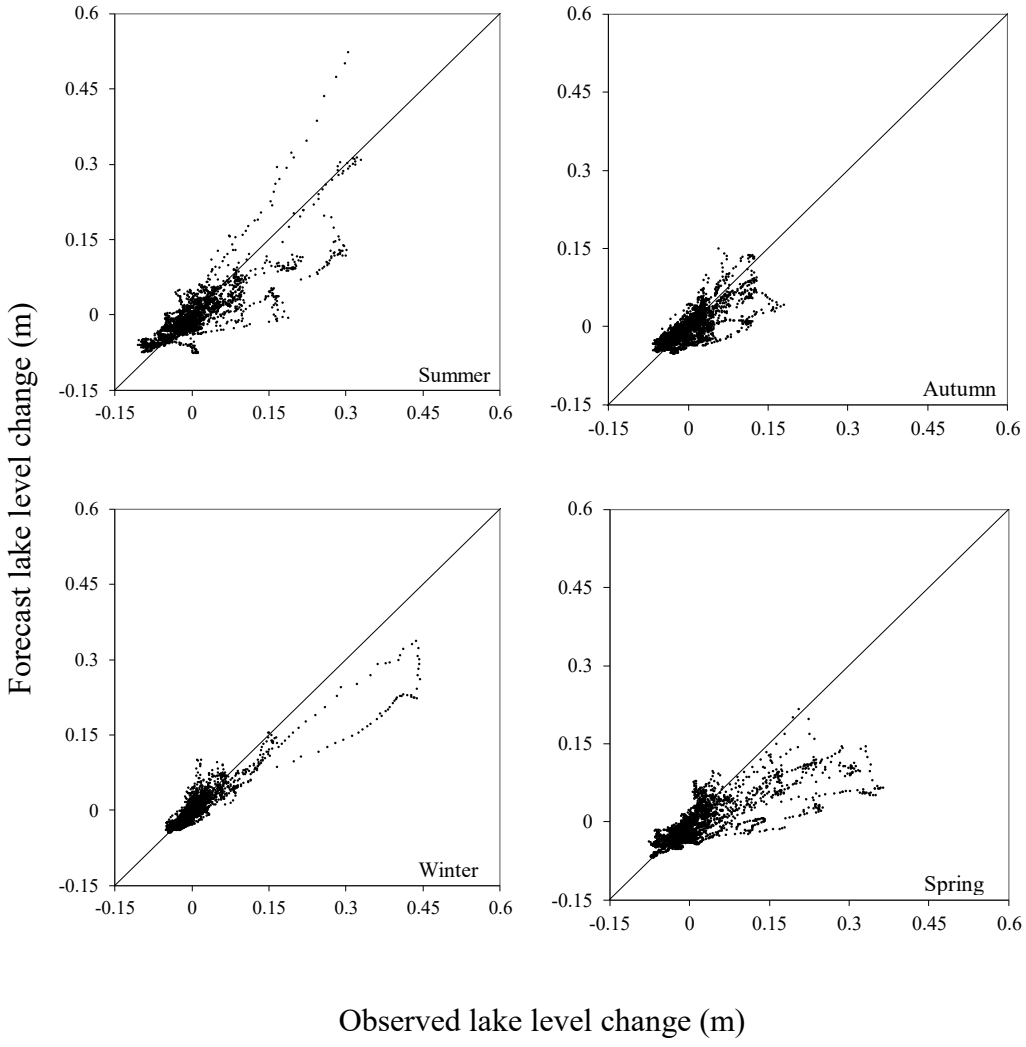

Figure 6-4: Seasonal scatterplots of the observed lake level changes against the forecast lake level changes at a lead-time of 48 hours for Lake Wakatipu for the forecast validation. The diagonal straight line is the 1:1 line.

Further inspecting the performance of the model through time series plots of ΔL_{48} and $\widehat{\Delta L}_{48}$ (Fig. 6-5 and 6-6) for forecast validation, it can be seen the model does well in following the general behaviour of the lake level changes in both lakes. In particular, correctly estimating the timing of lake level rises and lake level recession.

The large amount of scatter in $\widehat{\Delta L}_{48}$ appearing in the time series for the forecast validation is due to updating data at every time-step, which can make the forecast change in lake level change drastically with changing forecasts or the recording of heavy rain which was not in the forecast in the previous time-steps. For the calibration and hindcast validation, the data were not changed every run but simply moved across one relevant timestep, causing only small changes between adjacent $\widehat{\Delta L}_{48}$in the time-series.

The estimated lake level recession rates in the forecast validation followed the observed recessions well, although slightly underpredicting some of the more rapid recessions, as seen in January for both years and for both lakes. This underprediction of rapid lake level recession occurred in the hindcast validation also.

During November 2017, both the lakes were forecast to recede. However, Lake Wakatipu did not recede, and Lake Wanaka receded at a very low rate. This is likely due to high rates of snowmelt river water entering the lakes during this period, reducing the lakes recession rates (Fig. 6-5 and 6-6).

Inspecting the time series allows for evaluation of the model for estimating the smaller lake level rises. For both the lakes, several of these smaller rises are modelled particularly well with no clear overall under or over-prediction.

The larger lake level changes were almost all underpredicted, typical of most hydrograph model, apart from the obvious large over-prediction occurring on the last day of January and the beginning of February 2018. This particular lake level rise was a result of cyclone Fehi, which caused widespread flooding across much of the South Island of New Zealand and a state of emergency was declared in the Buller District on the West Coast (NIWA, 2017). As with the hindcast validation, the estimated lake level rise appears to follow the observed timing well, but magnitude prediction is not very accurate.

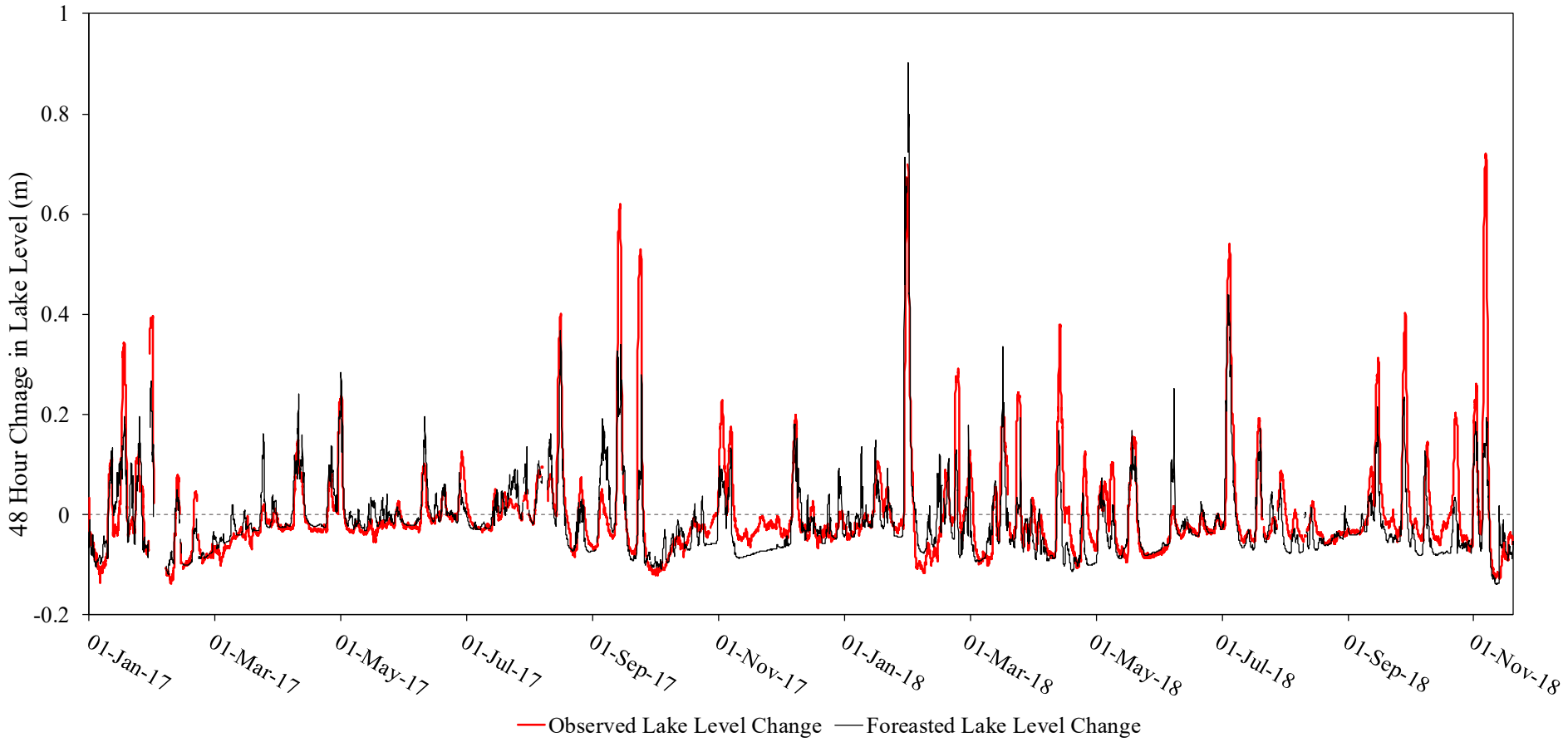

Figure 6-5: A time series plot of observed lake level change and the estimated lake level change, 48 hours ahead for Lake Wanaka, with predictions made every hour from January 1, 2017 to November 22, 2018, for the forecast validation.

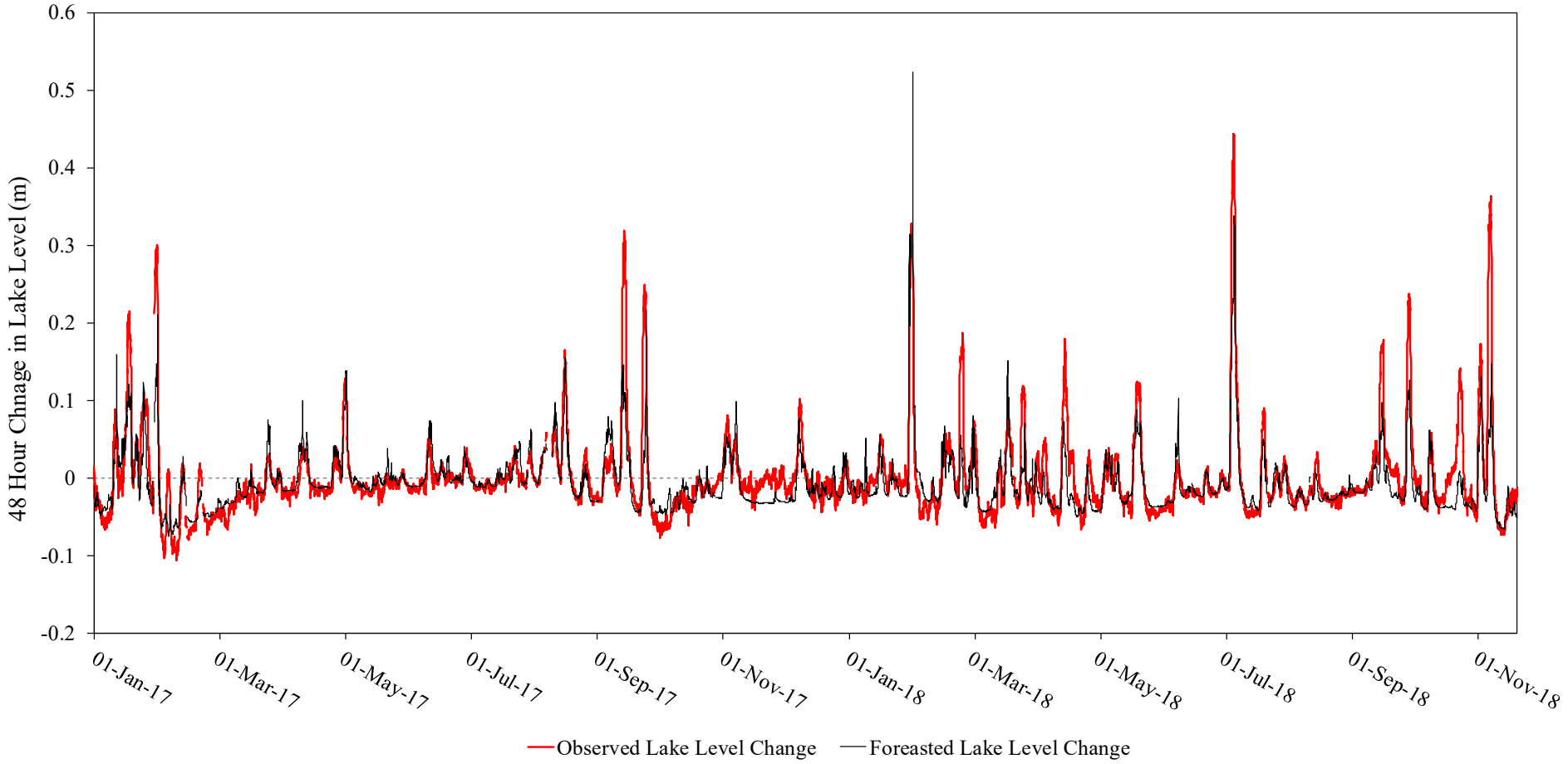

Figure 6-6: A time series plot of observed lake level change and the estimated lake level change, 48 hours ahead for Lake Wakatipu, with predictions made every hour from January 1, 2017 to November 22, 2018, for the forecast validation

Predictive Uncertainty

During operation the user of the model will need to understand the uncertainty of the model's deterministic outputs, as the uncertainty of predictions may influence decisions made from the model output (Beven, 2012). Using the observed lake level changes during the forecast validation period and the model output of forecast lake level changes at a lead-time of 48 hours, data was plotted showing the proportion of the observed lake level changes, from a model output range, that was equal to or below a lake level change value (Fig. 6-7 and 6-8).

For both lakes, if the model is forecasting for the lake to recede, $\widehat{\Delta L}_{48} < 0$, the proportion of observed values that receded is relatively high, for Lake Wanaka, it is ≈0.90 (Fig. 6-7) and for Lake Wakatipu it is ≈0.85 (Fig. 6-8). Therefore, the confidence of model recession is quite high. If the model output is $0 < \widehat{\Delta L}_{48} < 0.1$, the proportion of the observed lake level changes within that range is quite different for both the lakes. For Lake Wanaka the proportion of observed values less than the range was around ≈0.30 and a proportion ≈0.80 of observed lake level changes less than 0.1 m, making the proportion for the observed lake level changes falling within the range only ≈0.5. For Lake Wakatipu the proportion of observed values less than the range was around ≈0.15 and a proportion ≈0.90 of observed lake level changes less than 0.1 m, making the proportion of the observered lake levels to be within the range ≈0.75, much greater than Lake Wanaka.

The spread of the proportion of the observed lake level widens with increasing forecast lake level rise, reflecting an increase in uncertainty with increasing forecast lake level rise. The overall underestimation in lake level rises, seen in the forecast validation results, is reflected in the proportion plots for the lakes. For example, if the model output for Lake Wanaka is $0.2 < \widehat{\Delta L}_{48} < 0.3$ only ≈ 0.45 of the observed lake levels were less than 0.3 m.

The selected ranges for the proportion plots are likely to be too small once the model is in operation, with higher ranges being required. Unfortunately, the forecast data set did not have many high forecast lake level changes and plotting the proportion of the few that did occur would be highly unreliable, as is already seen by the jaggedness in the curves in the overflow ranges, $0.3 < \widehat{\Delta L}_{48}$ for Lake Wanaka and $0.2 < \widehat{\Delta L}_{48}$ for Lake Wakatipu.

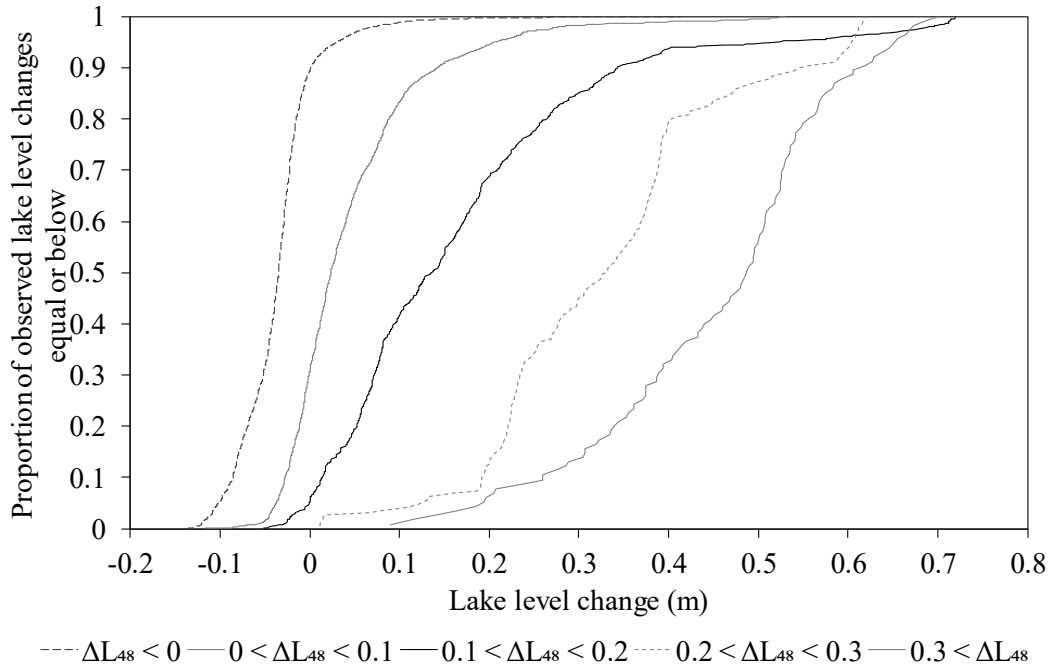

Figure 6-7: A plot showing the proportion of the observed lake level changes for Lake Wanaka, for a lead-time of 48 hours, for five different model estimation ranges in metres.

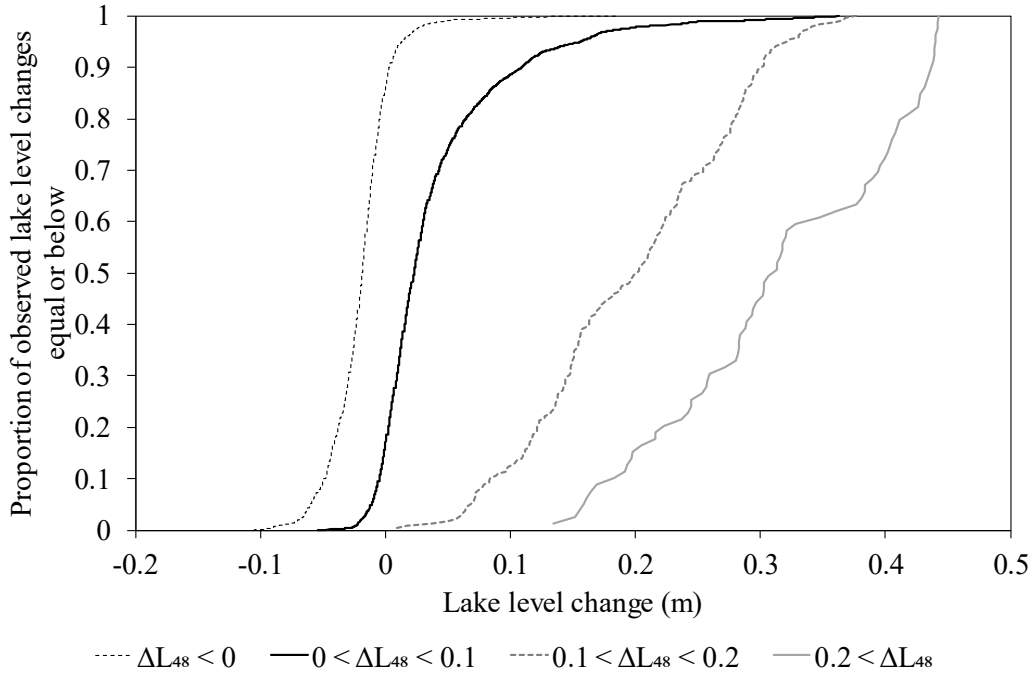

Figure 6-8: A plot showing the proportion of the observed lake level changes for Lake Wakatipu, for a lead-time of 48 hours, for five different model estimation ranges in metres.

6.4 Lead-time performance

The model error was expected to increase over increasing lead-time for two main reasons, the first being that on average the lake level change over increasing lead-times increases and therefore so does the error that can be expected. The second reason being that the forecast rainfall 25 to 48 hours out had more associated error than the forecast rainfall 1 to 24 hours out, as seen in Figure 6-2. For both lakes the mean positive and mean negative residual errors have been plotted for each of the 48 lead-times in Figure 6-9. As expected, the error steadily increased with increasing lead-time.

For Lake Wanaka the error is around double that of Lake Wakatipu, this simply reflects the larger level change range experienced by Lake Wanaka. However, the lead-time error for Lake Wakatipu is around the same as Lake Wanaka for the first 1-4 hours, this is a result of the greater noise in the hourly lake level changes that Lake Wakatipu experiences.

The mean positive residual errors are about half that of the corresponding mean negative residual errors, this reflects that the model is biaed towards underestimation which has been clearly demonstrated throughout the forecast model evaluation.

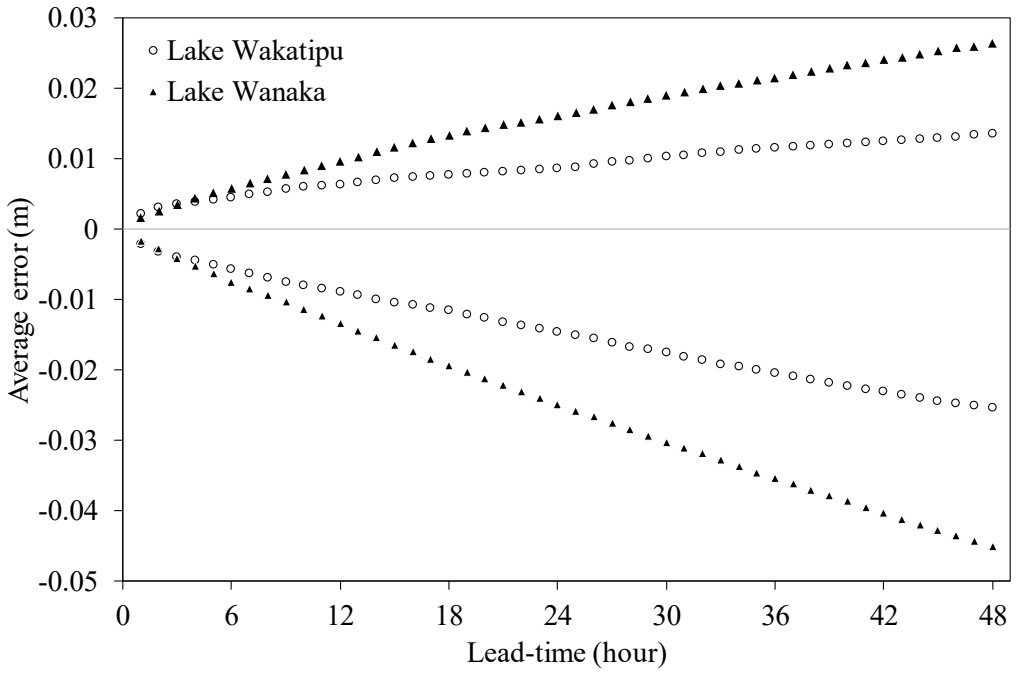

Figure 6-9: The average negative and positive residual errors from the forecast validation, across all 48 lead-times, for both Lakes Wanaka and Wakatipu.

6.5 Forecast validation quality

The results from the forecast validation show the model underestimates most lake level rises and does reasonably well estimating the lake level recessions, although tends to underestimate the more rapid lake level recessions. However, the quality of this forecast validation must be acknowledged and is hindered in many ways as will be discussed.

The year 2017 was very dry year for the South Island, New Zealand with Cromwell experiencing its 3rd lowest annual total of rainfall since records began in 1949 (NIWA, 2018), making it a poor year for the model validation as it is not representative of normal years and much drier than any of the years in the calibration period.

Over the whole forecast validation period from January to 2017 to November 2018, Lake Wanaka only recorded three lake level rises over 0.6 m, two of which occurred in spring, while for the hindcast validation period the lake experienced nine lake level rises exceeding 0.6 m, with at least one occurring in each of the seasons. This suggests that for many of the results presented in this chapter, (which placed emphasis on model error, such as the yearlong NSE value) the probability plots and the lead-time errors are more representative of the model performance in spring rather than all four seasons.

The third lake level rise of over 0.6 m for Lake Wanaka, during the forecast validation period, was due to Cyclone Fehi occurring at the beginning of February 2018. This rise was greatly over-predicted by the model. This is because Cyclone Fehi was an abnormal weather event and therefore the forecast rainfall would have been subject to larger than normal errors. The rain gauge recordings during this event would have also been poorly representative of the rainfall in the catchment due to the large spatial variability of rainfall during such extreme events.

While it is useful to have some weather extremes during a validation period which fall outside of calibrated range of values, it is not useful for model evaluation to validate on a time period which is not representative of the normal patterns at all. It may be that the model performs better than the results suggested.

The results also showed a clear theme of underprediction for lake level rise across all seasons, with the exception of the large lake level rise resulting from Cyclone Fehi. This implies the ω_f may be too low and there may be a need for further

investigation of the correlation between forecast and recorded rainfall. The error of forecast and recorded rainfall during Cyclone Fehi may have skewed the calculation of ω_f. It could be that the relationship between forecast rainfall depth and recorded rainfall depth is not a simple linear relationship, with the weight given to the forecast rainfall needing to be different for small events and large events.

A model developed and calibrated on recorded rainfall data is not typically to be run with forecast rainfall data and if so a recalibration of the model is needed. Li *et al.* (2017) recalibrated a forecast hydrological model calibrated on recorded rainfall data with forecast rainfall data. The recalibration of the model improved the model performance, with the NSE at a 24 hour lead time improving from 0.75, pre-recalibration, to 0.78, post-recalibration, and for a 48 hour lead time improving from 0.64, pre-recalibration, to 0.72, post-recalibration. This example shows there is potential for model improvement if the lake level change model were to be recalibrated on forecast rainfall data.

6.6 Conclusion

The forecast validation required the correlation between forecast rainfall and recorded rainfall to be calculated and applied to the forecast rainfall prior to being input in the model. The forecast temperature was also adjusted to the same elevation of the recorded temperature data. The forecast validation was run over the period from January 2017 to November 2018 and showed the model does fairly well estimating the timing of lake level changes. However, there is some error in the magnitude of the estimates. The model is subject to underestimation of most large lake level rises and for smaller rises the model is more accurate, although still subject to over and underestimation.

The results from the forecast validation are helpful to enable the model user to know the predictive uncertainty of the model, although this will be more uncertain for large events.

Chapter 7 - Conclusion

The Clutha river, situated in the southeast section of the South Island, New Zealand, has two hydro-power stations, the Clyde Dam and downstream the Roxburgh Dam, with a generating capacity of 432 MW and 320 MW, respectively. The two hydro-power stations are operated by Contact Energy, providing around 10% of New Zealand's electrical energy.

To maintain operational efficiency of the hydro-power stations Contact Energy requires forecasts of the hourly inflows into the head-pond lake of the Clyde Dam, Lake Dunstan. The current inflow forecast model, operated by Contact Energy, routes many forecast flows from sub-catchments upstream of Lake Dunstan. The model is subject to some degree of predictive error. However, it has been identified that improving the accuracy of the forecast levels of Lakes Wanaka and Wakatipu may reduce the error of the inflow model. The aim of this thesis was to as accurately as possible forecast the levels of Lakes Wanaka and Wakatipu. The end-goal is for improved operational lake outflow forecasts from these lakes, for routing into Lake Dunstan.

The first objective to achieve the aim was to develop a forecast lake level model with a lead-time out to 48 hours. This was achieved by developing an empirical lake level change forecast model, using rainfall, temperature, and current lake level as independent variables. The developed model has two main components, the first component estimates the lake level recession rates based on the current lake level. This assumes influences of variations in river baseflow inflows into a lake have negligible impact on the lake level recession rates.

The second part of the model estimates the lake rise resulting from recent rainfall in the catchment. It does this by computing lake level rise hydrographs for effective rainfall using the inverse Gaussian distribution to represent the hydrograph form. The outputs from the two components are added together to estimate the actual lake level change for hourly lead-times out to 48 hours.

The lake level forecast model was developed and calibrated using recorded data, and first evaluated also using recorded data on the years 2015 – 2016 (hindcast validation). For the lead-time of 48 hours the model was shown to perform reasonably well, closely estimating the time distribution of positive lake level

changes and lake level recessions. As with most hydrograph models, the model underpredicted many of the peak positive lake level changes, more so in Lake Wanaka than Lake Wakatipu. For the hindcast validation for both lakes, the model performed least accurately during spring, predominantly underestimating positive lake level changes. Given that the model does not have a snowmelt component this was not surprising. The model also tended to underestimate some of the rapid lake level recession rates for both lakes, following significant inflow events.

The hindcast validation results illustrate some limitations of the model when using rain gauge rainfall. This arises because an assumption of the model is that rain gauge rainfall is representative of spatially averaged catchment rainfall over short time periods. This is most often not the case. In the hindcast validation period Lake Wakatipu experienced a large lake level rise event which the model failed to predict. The likely explanation is that the catchment of Lake Wakatipu was receiving rainfall in areas other than the rain gauge area. This highlights uncertainty of the recorded rain gauge rainfall being representative of the whole catchment, which will lead to errors in the model outputs for any predictive model.

The second objective of this thesis was to evaluate the developed model's performance using forecast rainfall and temperature data, referred to as the forecast validation. This essentially estimated how the model will perform when in operation, where only forecast data are being used for model inputs.

The first step to perform the forecast validation was to correlate forecast rainfall to the recorded rainfall and secondly, using the forecast temperature lapse rate, adjust the forecast temperature to the same elevation as the catchment recorded temperature. The forecast validation was carried out from January 2016 to November 2017, the results of the validation show a large additional error introduced to the model via the use of weather-based forecasts of rainfall and temperature.

Most of the time, the forecast rainfall was able to accurately predict the presence of rainfall within the lake catchments, transferring to the model accurately estimating the times of positive or negative lake level changes. However, the model lost accuracy, relative to the hindcast validation, when estimating the magnitude of the lake level rises. The greater the estimated positive lake level change the greater the amount of error, tending towards underestimation.

The model underestimated the relatively few rapid lake level recessions in the forecast validation but performed reasonably when estimating most lake level recessions. Once more the model performed worst in spring, underestimating the positive lake level changes and overestimated recession rates, likely due to the snowmelt contributions.

Overall the forecast validation showed the model is capable of estimating lake level changes with a higher degree of accuracy than the benchmark model of no lake level change. The model is capable of estimating lake level recession with a reasonabe degree of accuracy in recession rates and is capable of estimating positive lake level changes, but lacking accuracy in the estimate of the lake level rise magnitude. While not perfect, as with any hydrological model, the model has shown to be able to reasonably forecast lake level changes in an operational situation, given the uncertainties associated with forecast rainfall.

The quality of the performance evaluation of the model using forecast data has some level of uncertainty itself. This is because the time period of the validation had low rainfall, with relatively few lake level rise events. The few large events which did occur were in spring, which has been demonstrated to be the most difficult season for lake level change prediction. The validation period also experienced an ex-tropical cyclone, Cyclone Fehi, which is not a typical event in the longer time series.

The following recommendations are suggested for future research toward increasing the accuracy of forecast lake levels:

- *Recalibrate the model on forecast data:* When using forecast rainfall as an input into the model instead of recorded rainfall a source of error is introduced, other than the error in the forecast data itself. This is because the model was developed and calibrated on recorded rain gauge and temperature data. An adjustment of the model parameters when using forecast data may improve the model's predictability as has been the case in other studies. It will also eliminate the need for the use of the correlation between the recorded rainfall and forecast rainfall, reducing any error sourced from it.

- *Add a subroutine for estimating snow accumulation and snowmelt:* At present the model does not estimate snow accumulation and snowmelt. It does reduce runoff rates due to snow accumulation but does not convert this to snow storage. To add a snow routine to the model, a record of the catchment spatial

temperature would be required for development of the routine and a record of snow observations would be required to validate the routine. The use of a snow routine may help to more accurately estimate lake level changes occurring in spring and early summer.

- *Investigate the use of other sources of rainfall inputs:* The current model makes use of just two rain gauges for each lake to represent the average catchment rainfall. Improving the estimate of average catchment rainfall to have occurred will improve the model's accuracy of forecasting shorter lead-times lake level changes, cascading out to an improvement of the accuracy at 48 hours.

  Improvements in estimating average catchment rainfall may come from using rain gauge recordings from rain gauges closer to the Main Divide. While there are no telemetric hourly rain gauges on the eastern side of the Main Divide, using one at high elevations on the western side of the Main Divide may prove useful.

  Radar and satellite recordings of recent rainfall in the catchment may also help improve the estimation of the catchment spatial average rainfall. The two sources estimate the spatial distribution of rainfall well and will better capture periods of time where rainfall is occurring in the catchment non-uniformly. The issue arises with the conversion of the radar and satellite data to give an estimate of rainfall rate. However, this is fast developing field and may soon be able help improve lake level forecasts.
- *Climate change:* the model has been calibrated for present climate conditions and rainfall patterns. Change in climate conditions may affect how well the model estimates lake level changes. The model has already been shown to fail to estimate lake level changes in the presence of a rainfall anomaly, an ex-tropical cyclone. Similarly, a change in the average rainfall patterns may require the model to be recalibrated.

In conclusion, a lumped hydrological model has been developed to be applied to Lakes Wanaka and Wakatipu. The model performs reasonably well when consideration for the uncertainties associated with forecast rainfall and the limited rain gauges is taken into account. It is recommended the model be recalibrated on forecast rainfall data as soon as more records become available. In the meantime, the model may be put into operational use, helping forecast inflows into Lake Dunstan.

References

Aronica, G., Freni, G., & Oliveri, E. (2005). Uncertainty analysis of the influence of rainfall time resolution in the modelling of urban drainage systems. *Hydrological Processes: An International Journal, 19*(5), 1055-1071.

Bardsley, E. (2015). Goodness of fit indices for discharge forecasts in real time. *Journal of Hydrology (New Zealand), 54*(1), 23-26.

Bardsley, W. (1983). An alternative distribution for describing the instantaneous unit hydrograph. *Journal of Hydrology, 62*(1-4), 375-378.

Bardsley, W. E., Vetrova, V., & Liu, S. (2015). Toward creating simpler hydrological models: A LASSO subset selection approach. *Environmental Modelling & Software, 72*, 33-43.

Bergström, S., & Forsman, A. (1973). Development of a conceptual deterministic rainfall-runoff model. *Nordic Hydrology, 17*(4), 147-170.

Beven, K. (2002a). Towards a coherent philosophy for modelling the environment. *Proceedings of the Royal Society a-Mathematical Physical and Engineering Sciences, 458*(2026), 2465-2484.

Beven, K. (2002b). Towards an alternative blueprint for a physically based digitally simulated hydrologic response modelling system. *Hydrological Processes, 16*(2), 189-206.

Beven, K. (2013). So how much of your error is epistemic? Lessons from Japan and Italy. *Hydrological Processes, 27*(11), 1677-1680.

Beven, K. J. (2012). *Rainfall-runoff modelling : the primer*. Chichester, West Sussex; Hoboken, NJ: Wiley-Blackwell.

Biondi, D., Freni, G., Iacobellis, V., Mascaro, G., & Montanari, A. (2012). Validation of hydrological models: Conceptual basis, methodological approaches and a proposal for a code of practice. *Physics and Chemistry of the Earth, Parts A/B/C, 42-44*, 70-76.

Bottomley, G. A. (1955). Seiches on Lake Wakatipu, New Zealand. *Royal Society of New Zealand, 83*, 579-587.

Boyle, D. P., Gupta, H. V., & Sorooshian, S. (2000). Toward improved calibration of hydrologic models: Combining the strengths of manual and automatic methods. *Water Resources Research, 36*(12), 3663-3674.

Chinn, T. (1979). How wet is the wettest of the wet West Coast. *New Zealand Alpine Journal, 32*, 85-88.

Chow, V. T., Maidment, D. R., & Mays, L. W. (1988). *Applied hydrology*. (Vol. 308). New York: McGraw Hill Book Company.

Cloke, H. L., & Pappenberger, F. (2009). Ensemble flood forecasting: A review. *Journal of Hydrology, 375*(3), 613-626.

Collischonn, W., Haas, R., Andreolli, I., & Tucci, C. E. M. (2005). Forecasting River Uruguay flow using rainfall forecasts from a regional weather-prediction model. *Journal of Hydrology, 305*(1), 87-98.

Cuo, L., Pagano, T. C., & Wang, Q. J. (2011). A Review of Quantitative Precipitation Forecasts and Their Use in Short- to Medium-Range Streamflow Forecasting. *Journal of Hydrometeorology, 12*(5), 713-728.

Dawson, C., & Wilby, R. (2001). Hydrological modelling using artificial neural networks. *Progress in physical Geography, 25*(1), 80-108.

Devi, G. K., Ganasri, B. P., & Dwarakish, G. S. (2015). A Review on Hydrological Models. *Aquatic Procedia, 4*, 1001-1007.

Dong, X., Dohmen-Janssen, C. M., & Booij, M. J. (2005). Appropriate Spatial Sampling of Rainfall or Flow Simulation/Echantillonnage Spatial de la Pluie Approprié pour la Simulation D'écoulements. *Hydrological Sciences Journal, 50*(2), 279 - 298.

Duan, Q., Gupta, H. V., Sorooshian, S., Rousseau, A., & Turcotte, R. (2004). *Calibration of watershed models*. Washington DC: American Geophysical Union.

Duncan, M. R., Austin, B., Fabry, F., & Austin, G. L. (1993). The effect of gauge sampling density on the accuracy of streamflow prediction for rural catchments. *Journal of Hydrology, 142*(1), 445-476.

Fitzharris, B. (1992). The 1992 electricity crisis and the role of climate and hydrology. *New Zealand Geographer, 48*(2), 79-83.

Fitzharris, B. B., & Garr, C. E. (1995). Simulation of past variability in seasonal snow in the Southern Alps, New Zealand. *Annals of Glaciology, 21*, 377-382.

Freeze, R. A., & Harlan, R. L. (1969). Blueprint for a physically-based, digitally-simulated hydrologic response model. *Journal of Hydrology, 9*(3), 237-258.

Ghorbani, M. A., Singh, V. P., Sivakumar, B., Kashani, M. H., Atre, A. A., & Asadi, H. (2017). Probability distribution functions for unit hydrographs with optimization using genetic algorithm. *Applied Water Science, 7*(2), 663-676.

Gragne, A. S., Alfredsen, K., Sharma, A., & Mehrotra, R. (2015a). Recursively updating the error forecasting scheme of a complementary modelling framework for improved reservoir inflow forecasts. *Journal of Hydrology, 527*, 967-977.

Gragne, A. S., Sharma, A., Mehrotra, R., & Alfredsen, K. (2015b). Improving real-time inflow forecasting into hydropower reservoirs through a complementary modelling framework. *Hydrol. Earth Syst. Sci., 19*(8), 3695-3714.

Habets, F., LeMoigne, P., & Noilhan, J. (2004). On the utility of operational precipitation forecasts to served as input for streamflow forecasting. *Journal of Hydrology, 293*(1), 270-288.

Hosseini, M., & Aqeel Ashraf, M. (2015). Application of Hydrological Models Related to Land Use Land Cover Change. In *Application of the SWAT Model for Water Components Separation in Iran* (pp. 1-32). New York, USA: Springer.

Jain, S. K., & Sudheer, K. P. (2008). Fitting of hydrologic models: A close look at the Nash-Sutcliffe index. *Journal of Hydrologic Engineering, 13*(10), 981-986.

Jakeman, A. J., & Hornberger, G. M. (1993). How much complexity is warranted in a rainfall-runoff model. *Water Resources Research, 29*(8), 2637-2649.

Kerr, T. (2013). The contribution of snowmelt to the rivers of the South Island, New Zealand. *Journal of Hydrology (New Zealand), 52*(2), 61-82.

Kirchner, J. W. (2006). Getting the right answers for the right reasons: Linking measurements, analyses, and models to advance the science of hydrology. *Water Resources Research, 42*(3), 1 - 5.

Klemeš, V. (1986). Operational testing of hydrological simulation models. *Hydrological Sciences Journal, 31*(1), 13-24.

Kobold, M. (2005). Precipitation forecasts and their uncertainty as input into hydrological models. *Hydrology and Earth System Sciences Discussions, 9*(4), 322-332.

Kokkonen, T. S., & Jakeman, A. J. (2001). A comparison of metric and conceptual approaches in rainfall - runoff modeling and its implications. *Water Resources Research, 37*(9), 2345-2352.

Krajewski, W. F., Ciach, G. J., & Habib, E. (2003). An analysis of small-scale rainfall variability in different climatic regimes. *Hydrological sciences journal, 48*(2), 151-162.

Krause, P., Boyle, D., & Bäse, F. (2005). Comparison of different efficiency criteria for hydrological model assessment. *Advances in Geosciences, 5*, 89-97.

Kuczera, G., Kavetski, D., Franks, S., & Thyer, M. (2006). Towards a Bayesian total error analysis of conceptual rainfall-runoff models: Characterising model error using storm-dependent parameters. *Journal of Hydrology, 331*(1-2), 161-177.

Lees, M., Young, P. C., Ferguson, S., Beven, K., & Burns, J. (1994). An adaptive flood warning scheme for the River Nith at Dumfries. In *International Conference on River Flood Hydraulics* (2 ed., pp. 65-75). Chichester, England: John Wiley and Sons Ltd.

Li, J., Chen, Y. B., Wang, H. Y., Qin, J. M., Li, J., & Chiao, S. (2017). Extending flood forecasting lead time in a large watershed by coupling WRF QPF with a distributed hydrological model. *Hydrology and Earth System Sciences, 21*(2), 1279-1294.

Lindström, G., Johansson, B., Persson, M., Gardelin, M., & Bergström, S. (1997). Development and test of the distributed HBV-96 hydrological model. *Journal of hydrology, 201*(1-4), 272-288.

Macara, G. R. (2015). *The climate and weather of Otago.* National Institute of Water and Atmospheric Research. 44p. Retrieved August 2017, from http://docs.niwa.co.nz/library/public/NIWAsts67.pdf.

McMillan, H., Jackson, B., Clark, M., Kavetski, D., & Woods, R. (2011). Rainfall uncertainty in hydrological modelling: An evaluation of multiplicative error models. *Journal of Hydrology, 400*(1), 83-94.

Mendez, M., & Calvo-Valverde, L. (2016). Development of the HBV-TEC Hydrological Model. *Procedia Engineering, 154*, 1116-1123.

Merz, B., & Thieken, A. H. (2005). Separating natural and epistemic uncertainty in flood frequency analysis. *Journal of Hydrology, 309*(1), 114-132.

Ministry for the Environment. (2016). *Average annual rainfall, 1972-2013*. Retrieved January 2019, from https://data.mfe.govt.nz/layer/89420-average-annual-rainfall-2016/.

Ministry of Business Innovation & Employment. (2018). *Electricity Statistics.* Retrieved November 2018, from https://www.mbie.govt.nz/building-and-energy/energy-and-natural-resources/energy-statistics-and-modelling/energy-statistics/electricity-statistics/.

Mohssen, M., & Goldsmith, M. (2011). Flood forecasting of lake levels: A new concept. *International Journal of Safety and Security Engineering, 1*(4), 363-375.

Murray, D. L. (1975). Regional hydrology of the Clutha River. *Journal of Hydrology (New Zealand), 14*(2), 83-98.

Nash, J. E., & Sutcliffe, J. V. (1970). River flow forecasting through conceptual models part I — A discussion of principles. *Journal of Hydrology, 10*(3), 282-290.

National Institute of Water and Atmospheric Research. (2017). *Climate Summary February 2017.* 13p. Retrieved November 2018, from https://www.niwa.co.nz/files/Climate_Summary_February_2017.pdf.

National Institute of Water and Atmospheric Research. (2018). *Climate Summary for 2017.* 36p. Retrieved November 2018, from https://www.niwa.co.nz/sites/niwa.co.nz/files/2017_Annual_Climate_Summary_FINAL2.PDF.

Perrin, C., Michel, C., & Andreassian, V. (2001). Does a large number of parameters enhance model performance? Comparative assessment of common catchment model structures on 429 catchments. *Journal of Hydrology, 242*(3-4), 275-301.

Perrin, C., Michel, C., & Andréassian, V. (2003). Improvement of a parsimonious model for streamflow simulation. *Journal of Hydrology, 279*(1), 275-289.

Poyck, S., Hendrikx, J., McMillan, H., Hreinsson, E. Ö., & Woods, R. (2011). Combined snow and streamflow modelling to estimate impacts of climate change on water resources in the Clutha River, New Zealand. *Journal of Hydrology (New Zealand), 50*(2), 293-311.

Quick, M. C., & Pipes, A. (1977). UBC watershed model. *Hydrological Sciences Journal, 22*(1), 153-161.

Renard, B., Kavetski, D., Kuczera, G., Thyer, M., & Franks, S. W. (2010). Understanding predictive uncertainty in hydrologic modeling: The challenge of identifying input and structural errors. *Water Resources Research, 46*(5), 1 - 22.

Roulin, E., & Vannitsem, S. (2005). Skill of medium-range hydrological ensemble predictions. *Journal of Hydrometeorology, 6*(5), 729-744.

Roy, A., & Thomas, R. (2016). A Comparative Study on the Derivation of Unit Hydrograph for Bharathapuzha River Basin. *Procedia Technology, 24*, 62-69.

Schaefli, B., & Gupta, H. V. (2007). Do Nash values have value? *Hydrological Processes: An International Journal, 21*(15), 2075-2080.

Schaefli, B., Hingray, B., Niggli, M., & Musy, A. (2005). A conceptual glacio-hydrological model for high mountainous catchments. *Hydrology and Earth System Sciences Discussions, 9*, 95-109.

Schilling, W. (1991). Rainfall data for urban hydrology: what do we need? *Atmospheric Research, 27*(1-3), 5-21.

Sinclair, M. R., Wratt, D. S., Henderson, R. D., & Gray, W. R. (1997). Factors affecting the distribution and spillover of precipitation in the Southern Alps of New Zealand—A case study. *Journal of Applied Meteorology, 36*(5), 428-442.

Sivakumar, B. (2008a). Dominant processes concept, model simplification and classification framework in catchment hydrology. *Stochastic Environmental Research and Risk Assessment, 22*(6), 737-748.

Sivakumar, B. (2008b). The more things change, the more they stay the same: the state of hydrologic modelling. *Hydrological Processes, 22*(21), 4333-4337.

Sivapalan, M., Blöschl, G., Zhang, L., & Vertessy, R. (2003). Downward approach to hydrological prediction. *Hydrological processes, 17*(11), 2101-2111.

Sun, X., Mein, R. G., Keenan, T. D., & Elliott, J. F. (2000). Flood estimation using radar and raingauge data. *Journal of Hydrology, 239*(1), 4-18.

Taylor, M., & Bardsley, E. (2015). The Interdecadal Pacific Oscillation and the Southern Oscillation Index: relative merits for anticipating inflows to the Upper Clutha lakes. *Journal of Hydrology, 54*(2), 67.

Todini, E. (1988). Rainfall-runoff modeling—Past, present and future. *Journal of Hydrology, 100*(1-3), 341-352.

Todini, E. (2007). Hydrological catchment modelling: past, present and future. *Hydrology and Earth System Sciences, 11*(1), 468-482.

Todini, E. (2011). History and perspectives of hydrological catchment modelling. *Hydrology Research, 42*(2-3), 73-85.

Tweedie, M. C. (1957). Statistical properties of inverse Gaussian distributions. I. *The Annals of Mathematical Statistics, 28*(2), 362-377.

Villarini, G., Mandapaka, P. V., Krajewski, W. F., & Moore, R. J. (2008). Rainfall and sampling uncertainties: A rain gauge perspective. *Journal of Geophysical Research: Atmospheres, 113*(D11).

Wagener, T., Boyle, D. P., Lees, M. J., Wheater, H. S., Gupta, H. V., & Sorooshian, S. (2001). A framework for development and application of hydrological models. *Hydrology and Earth System Sciences Discussions, 5*(1), 13-26.

Wang, Y., He, B., & Takase, K. (2009). Effects of temporal resolution on hydrological model parameters and its impact on prediction of river discharge. *Hydrological Sciences Journal, 54*(5), 886-898.

Webby, M., & Waugh, J. (2006). Hydraulic behaviour of the outlet of Lake Wakatipu, Central Otago, New Zealand. *Journal of Hydrology (New Zealand), 45*(1), 29-40.